

CFD Modeling and AI-Based Prediction of Alkaline Water Electrolysis Cell's Performance for Hydrogen Production



By

Abdullah Sirat

(Registration No: 00000361132)

Department of Chemical Engineering

School of Chemical and Materials Engineering

National University of Sciences & Technology (NUST)

Islamabad, Pakistan

(2024)

CFD Modeling and AI-Based Prediction of Alkaline Water Electrolysis Cell's Performance for Hydrogen Production



By

Abdullah Sirat

(Registration No: 00000361132)

A thesis submitted to the National University of Sciences and Technology,
Islamabad, in partial fulfillment of the requirements for the degree of

Master of Science in Process Systems Engineering

Supervisor: Dr. Sher Ahmad

Co-Supervisor: Dr. Iftikhar Ahmad

School of Chemical and Materials Engineering
National University of Sciences and Technology (NUST)

H-12 Islamabad, Pakistan

2024



THESIS ACCEPTANCE CERTIFICATE

Certified that final copy of MS thesis written by **Abdullah Sirat** (Registration No 00000361132), of School of Chemical & Materials Engineering (SCME) has been vetted by undersigned, found complete in all respects as per NUST Statues/Regulations, is free of plagiarism, errors, and mistakes and is accepted as partial fulfillment for award of MS degree. It is further certified that necessary amendments as pointed out by GEC members of the scholar have also been incorporated in the said thesis.

Signature: _____

Name of Supervisor: Dr. Sher Ahmad

Date: _____

for Signature (HOD): _____

Date: 19/04/24

Signature (Dean/Principal): _____

Date: 19.4.2024

National University of Sciences & Technology (NUST)

MASTER'S THESIS WORK

Formulation of Guidance and Examination Committee (GEC)

Name: Abdullah Sirat NUST Reg No: 00000361132
 Department: Department of Chemical Engineering Specialization: Master of Science in Process System Engineering
 Credit Hour Completed: 24.0 CGPA: 3.81

Course Work Completed

S/No:	Code:	Title:	Core/Elective:	CH:	Grade:
1.	PSE-801	Process Systems Theory	Compulsory	3.0	A
2.	PSE-852	Process Modelling and Simulation	Compulsory	3.0	B+
3.	TEE-820	Process Intensification	Elective	3.0	A
4.	RM-898	Research Methodology	Additional	2.0	Q
5.	PSE-823	Advanced Process Dynamics and Control	Compulsory	3.0	B+
6.	PSE-802	Optimization and Decision Analysis	Compulsory	3.0	B+
7.	CSE-801	Computational Fluid Dynamics	Elective	3.0	A
8.	ENE-809	Waste Water Treatment & Design	Elective	3.0	A
9.	EME-902	Numerical Methods In Chemical Engineering	Elective	3.0	A

Date 02 - Feb - 2023

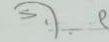
Student's Signature



Thesis Committee

Name: Sher Ahmad (Supervisor)
 Department: Department of Chemical Engineering

Signature



Name: Iftikhar Ahmad (Cosupervisor)
 Department: Department of Chemical Engineering

Signature



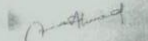
Name: Muhammad Ahsan (Internal)
 Department: Department of Chemical Engineering

Signature

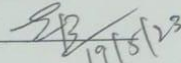


Name: Dr. Nouman Ahmad (Internal)
 Department: Department of Chemical Engineering

Signature

Date: 02 - Feb - 2023

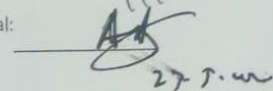
Signature of Head of Department:



APPROVAL

Date: 02 - Feb - 2023

Signature of Dean/Principal:





Form: TH-04

National University of Sciences & Technology (NUST)

MASTER'S THESIS WORK

We hereby recommend that the dissertation prepared under our supervision by

Regn No & Name: 00000361132 Abdullah Sirat

Title: CFD Modeling and AI-Based Prediction of Alkaline Water Electrolysis Cell Performance for Hydrogen Production.

Presented on: 14 Mar 2024 at: 1500 hrs in SCME (Seminar Hall)

Be accepted in partial fulfillment of the requirements for the award of Master of Science degree in Process Systems Engineering.

Guidance & Examination Committee Members

Name: Dr Muhammad Ahsan

Signature: [Signature]

Name: Dr Nouman Ahmad

Signature: [Signature]

Name: Dr Iftikhar Ahmad (Co-Supervisor)

Signature: [Signature]

Supervisor's Name: Dr Sher Ahmad

Signature: [Signature]

Dated: 13-03-2024

[Signature]
Head of Department

Date 4/4/24

[Signature]
Dean/Principal

Date 5-4-2024

School of Chemical & Materials Engineering (SCME)

AUTHOR'S DECLARATION

I Abdullah Sirat hereby state that my MS thesis titled “CFD Modeling and AI-Based Prediction of Alkaline Water Electrolysis Cell’s Performance for Hydrogen Production” is my own work and has not been submitted previously by me for taking any degree from the National University of Sciences and Technology, Islamabad, or anywhere else in the country/world.

At any time, if my statement is found to be incorrect even after I graduate, the university has the right to withdraw my MS degree.

Name: Abdullah Sirat

Date: 14-03-2024

PLAGIARISM UNDERTAKING

I solemnly declare that the research work presented in the thesis titled “CFD Modeling and AI-Based Prediction of Alkaline Water Electrolysis Cell’s Performance for Hydrogen Production” is solely my research work with no significant contribution from any other person. Small contribution/ help wherever taken has been duly acknowledged and that complete thesis has been written by me.

I understand the zero-tolerance policy of the HEC and the National University of Sciences and Technology (NUST), Islamabad towards plagiarism. Therefore, I as an author of the above-titled thesis declare that no portion of my thesis has been plagiarized and any material used as reference is properly referred to/cited.

I undertake that if I am found guilty of any formal plagiarism in the above-titled thesis even after the award of my MS degree, the University reserves the right to withdraw/revoke my MS degree and that HEC and NUST, Islamabad has the right to publish my name on the HEC/University website on which names of students are placed who submitted plagiarized thesis.

Name: Abdullah Sirat

Date: 14-03-2024

DEDICATION

By the grace of **Almighty Allah**, who is the most Compassionate and Merciful.

With heartfelt dedication, I offer this achievement to **my Parents**, whose unwavering love and support have fortified my journey. To my siblings, your unwavering encouragement has been my steadfast motivation.

To my exceptional supervisor, **Dr. Sher Ahmad**, your invaluable guidance has illuminated my path. To my esteemed batch mates, your camaraderie and shared endeavors have enriched this journey.

This accomplishment stands as a testament to the collective contributions of everyone, inspiring me to continually strive for excellence.

ACKNOWLEDGEMENTS

All praise and eminence are due to "ALLAH," the unequivocal creator of this world, who bestowed upon us the gift of understanding and ignited our inquisitiveness about the entire universe. Warmest welcomes to the supreme ruler of this world and the hereafter, "Prophet Muhammed (PBUH)," a source of knowledge and benefits for all of humanity as well as for Ummah.

I would like to thank and convey my profound gratitude to my research **supervisor, Dr. Sher Ahmad** for his endless support, supervision, and guidance to steer me in the right direction whenever he thought I needed it. I would also like to convey gratitude to my **co-supervisor Dr. Iftikhar Ahmad** and **committee members; Dr. Muhammad Ahsan** and **Dr. Nouman Ahmad** for their invaluable suggestions and guidance.

Furthermore, I would also thank **Prof. Dr. Amir Azam Khan** (Principal School of Chemical and Materials Engineering) for providing a research-oriented platform to effectively utilize my efforts and skills in accomplishing this work. In the end, I want to express my profound gratitude to my parents for providing me their firm and constant support throughout my years of study, as well as during the research and writing of this thesis. This achievement would not have been attainable without their presence and guidance.

Abdullah Sirat

TABLE OF CONTENTS

ACKNOWLEDGEMENTS.....	ix
LIST OF FIGURES.....	xii
LIST OF TABLES.....	xiii
LIST OF ACRONYMS AND SYMBOLS.....	xiv
ABSTRACT.....	xvi
CHAPTER 1: INTRODUCTION.....	1
1.1 Background.....	1
1.2 Objectives.....	2
1.3 Thesis Outline.....	3
CHAPTER 2 LITERATURE REVIEW.....	4
2.1 Water electrolysis.....	4
2.2 Literature survey.....	5
CHAPTER 3: RESEARCH METHODOLOGY.....	8
3.1 Overview of Alkaline Water Electrolysis.....	8
3.2 Process Description and Model Development.....	10
3.3 Proposed Methodology.....	12
CHAPTER 4: CFD MODELING OF ALKALINE WATER ELECTROLYSIS AND DATA GENERATION.....	14
4.1 AWE CFD Modeling Setup and Parameters.....	14
4.1.1 Geometry and Discretization.....	14
4.2 Physical Modules and Governing Equations for CFD Simulations.....	16
4.2.1 Electric currents.....	17
4.2.2 Two-phase turbulent bubbly flow ($k - \epsilon$ model).....	19
4.3 Data Generation for ANN model.....	21
4.4 ANN Model Training and Validation.....	22
CHAPTER 5: ARTIFICIAL INTELLIGENCE MODEL ARCHITECTURE.....	23
5.1 Introduction to Artificial Intelligence and Machine Learning.....	23
5.2 Overview of Artificial Neural Networks.....	24
5.3 Architecture of the ANN Model.....	24
5.3.1 Input Layer.....	25
5.3.2 Hidden Layers.....	25
5.3.3 Output Layer.....	25

5.4 ANN Components	26
5.4.1 <i>Neurons</i>	26
5.4.2 <i>Weights</i>	26
5.4.3 <i>Biases</i>	26
5.4.4 <i>Activation Function</i>	26
CHAPTER 6: RESULTS AND DISCUSSION	28
6.1 CFD Modeling and Validation of AWE cell	28
6.2 Influence of operating parameters on the CFD model	28
6.2.1 <i>Influence of Temperature</i>	28
6.2.2 <i>Influence of Electrolyte weight concentration</i>	29
6.2.3 <i>Influence of Electrode-Diaphragm distance</i>	30
6.3 Gas Generation Profile	31
6.4 AWE Cell’s Performance Evaluation Using Artificial Neural Network	32
6.5 Analysis of ANN Model Accuracy and Validation	33
CHAPTER 7: CONCLUSION	35
REFERENCES	36

LIST OF FIGURES

Figure 3.1: Alkaline water electrolysis	9
Figure 3.2: Alkaline water electrolyzer structure	10
Figure 3.3: General schematic diagram of a single electrolysis cell including its outer components.....	11
Figure 3.4: A simplified representation of the AWE system	12
Figure 3.5: Flowchart of the proposed methodology	13
Figure 4.1: Mesh configuration of the cell	15
Figure 4.2: Compositions of the typical cell voltage of an AWE	19
Figure 5.1: Difference between AI, ML and DL	23
Figure 5.2: Architecture of multiple inputs and outputs ANN	25
Figure 6.1: Polarization curves for temperatures	29
Figure 6.2: Polarization curves for electrolyte weight concentration	30
Figure 6.3: Polarization curves for electrode-diaphragm distance	31
Figure 6.4: Gas distributions in the AWE cell	32
Figure 6.5: Regression plots of ANN model showing target vs. predicted values	33
Figure 6.6: Comparison Plots of ANN and CFD Model	34

LIST OF TABLES

Table 2.1: Comparison of different water electrolysis technologies based on parameters ...	5
Table 4.1: Geometric parameters	16
Table 4.2: Mesh statistics	16
Table 4.3: Model parameters for two-dimensional (2D) AWE cell	17

LIST OF ACRONYMS AND SYMBOLS

CFD	Computational Fluid Dynamics
AI	Artificial Intelligence
AWE	Alkaline Water Electrolysis
PEMWE	Proton Exchange Membrane Water Electrolysis
SOEC	Solid Oxide Electrolyzer Cell
ANN	Artificial Neural Network
ML	Machine Learning
DL	Deep Learning
SL	Supervised Learning
UL	Unsupervised Learning
MSE	Mean Square Error
RMSE	Root Mean Square Error
R_2	Coefficient of Determination
LMA	Levenberg Marquardt Algorithm
σ	Electrical Conductivity
\vec{J}_e	Externally Generated Current Density
Q_j	Current Source
$\frac{\partial \vec{D}}{\partial t}$	Electric Displacement
C	Concentration
T	Temperature
Φ_g	Volume Gas Fraction
τ_m	Tortuosity
ε_m	Porosity
U_{rev}	Reversible Voltage
ψ_T	Turbulent Viscosity
ψ_l	Dynamic Viscosity
\dot{m}_{gl}	Mass Transfer Rate
K	Turbulent Kinetic Energy
E	Turbulent Energy Dissipation

\vec{u}_g	Gas Velocity
n	Number of Samples
$Y_{i,pred}$	Predicted ANN Network
$Y_{i,CFD}$	CFD output
Y_{avg}	Average of Values
\vec{u}_l	Velocity Vector
F	Volumetric Force

ABSTRACT

This work presents a comprehensive model of an alkaline water electrolysis cell for hydrogen production to evaluate its electrochemical and fluid dynamic phenomena simultaneously. For this, a 2D alkaline water electrolysis model was simulated on COMSOL MULTIPHYSICS considering both gas and liquid phases. A Multiphysics approach is used in simulations and the results are validated with the experimental data to ensure model's accuracy. The CFD model includes the equations for electric current conservation and the gas and liquid phase. Polarization curves are generated to evaluate the AWE cell's performance and electrochemical response at different operating conditions. The CFD model allows to predict the distribution of the generated gases, movement of the bubbles, and turbulence within the cell as well as the impact of current density, electrolyte flow rate, electrode-diaphragm distance, and other parameters on the gas profiles. While the CFD model provides valuable insights into alkaline water electrolysis, combining it with a neural network model further enhances its potential for better cell design and performance. The trained ANN accurately predicted the complex relationships between input and output parameters with an R^2 value of 0.99922. The combined CFD-ANN approach provides comprehensive understanding of the AWE cell's behavior, further optimizing its design for efficient hydrogen production.

Keywords: hydrogen production, CFD modeling, experimental validation, ANN, climate change

CHAPTER 1: INTRODUCTION

1.1 Background

Tackling global warming and climate change are the key challenges in the 21st century. It is crucial to reduce the usage of fossil fuels and transition towards renewable energy in order to achieve carbon neutrality and meet the global energy demands [1]. From this perspective, green hydrogen is considered as a promising option due to its high efficiency and zero carbon emissions [2]. The green hydrogen's rise in popularity is due to the increased energy and fuel prices caused by limited oil supply and production, and the carbon dioxide emissions from the excess use of fossil fuels that contribute to climate change [3], [4]. Green hydrogen is utilized as a fuel in vehicles that consists of fuel cells to facilitate the decarbonization process within the transportation industry [5] and as a raw material in various industries including chemical industry and for the manufacturing of ammonia, thereby contributing significantly to the production of fertilizers [6]. The use of green hydrogen instead of fossil fuels could play a critical role towards achieving a future zero emissions and sustainability [7].

Solar and wind power are the two main sources of renewable energy for hydrogen production due to their widespread availability [8]. But the reliance of the renewable energy on the weather conditions and their local irregular distribution is a critical issue [9]. To avoid these issues, proper storage systems are required for energy, and the most possible option is the chemical energy carriers. Since hydrogen is produced more effectively by utilizing water electrolysis along with the excess renewable energy, thereby making it most promising option among others [9]. Hydrogen also has the ability to be effectively converted into electricity through fuel cells when needed, and utilized as a fuel in the transportation sector and industrial processes or fed back to the power grid [10]. This electrolysis process makes it possible to produce green hydrogen on a large scale and also store electrical energy [11].

The main technologies used commercially for green hydrogen production are alkaline, proton exchange membrane and solid oxide electrolysis. Alkaline water electrolysis involves water splitting technique for hydrogen production, in which electricity is passed between two electrodes to split water molecules into hydrogen and oxygen. AWE is a highly developed industrial technology and offers several advantages over others, such as durability, cost-effectiveness, longevity, and maturity [12]. The major barrier to green hydrogen's development in the energy industry is its high cost. Hydrogen produced from water electrolysis has a higher

production cost than the one produced from fossil fuels commonly known as blue hydrogen [13]. The two biggest drawbacks for alkaline water electrolysis are the challenges that arise from operating in dynamic environments and the low current densities [14]. Current density, over-voltage, efficiency, and other features of the electrolyzer are directly influenced by the properties of the materials such as catalysts, bipolar plates, and membranes [15]–[17].

Current density is the major cost contributor in most of electrolyzers and has the most effect on the size of electrolytic cell and capital cost. Due to these factors, the focus of research and development for electrolyzers is to increase the current density and resolve issues arising from operating in changing environments. Therefore, complex transport phenomena associated with multiphase flow is usually studied under different operating conditions and efforts are being made for modeling, and optimizing the design of alkaline water electrolysis in order to increase their efficiency and performance for green hydrogen production [18].

1.2 Objectives

This thesis aims to predict the performance of the alkaline water electrolysis (AWE) cell at different operating conditions such as temperature, electrolyte weight concentration and electrode-diaphragm distance, and provide insights into the electrochemical and fluid dynamic behavior of the cell. The main objectives of this thesis are listed below:

- Understanding the multiphase flow of the AWE cell.
- CFD Modeling of the AWE cell to study the electrochemical and fluid dynamic phenomena associated with the multiphase flow.
- Enhancing the performance of the cell by generating polarization curves (relates voltage and current density) at different conditions.
- Validation of the CFD model with experimental data using polarization curves to make sure the model is accurate.
- Developing large datasets through CFD simulation and develop an AI model capable of predicting the performance of the AWE cell.
- Integrate the CFD modeling with a data driven AI model to further enhance the model's abilities to predict the cell's behavior and performance under different operating conditions.

1.3 Thesis Outline

Chapter 1 gives a brief background of this research. Chapter 2 presents a comprehensive literature review of previously done research and fundamental concepts related to water electrolysis and its various technologies, particularly alkaline water electrolysis. Research methodology is discussed in chapter 3. In chapter 4, the CFD modelling of AWE cell, physical modules and their boundary conditions, and data generation for the ANN model are discussed. Chapter 5 presents a complete understanding of ANN, its architecture and components. The results of the CFD and AI model are discussed in Chapter 6, and conclusions are provided in Chapter 7 of the thesis.

CHAPTER 2 LITERATURE REVIEW

2.1 Water electrolysis

The issues of climate change and fossil fuels depletions demand immediate attention towards clean energy sources for sustainability. One promising way to achieve zero carbon emissions and meet the global energy demands is using hydrogen energy [19], [20]. The process of water electrolysis involves the splitting of water using electrical energy and it was first performed in 1789 by Deiman and van Troostwijk [21]. From these early experiments, various electrolysis methods have emerged, refined, and put into industrial practice over time.

The primary electrochemical method to produce hydrogen gas is water electrolysis and it holds a paramount status. Its importance keeps on increasing with the growth in renewable energy production. There are three main types of water electrolysis technologies, depending on many factors like temperature and pressure, types of electrolytes, electrodes and separators used. These include alkaline water electrolysis, proton exchange membrane water electrolysis and solid oxide electrolysis [22]. A comprehensive comparison of these water electrolysis technologies based on parameters is shown in Table 1.

Table 2.1 Comparison of different water electrolysis technologies based on the parameters [23]–[37].

Operating principle	AWE	PEMWE	SOEC
Cathode reaction	$2\text{H}_2\text{O} + 2\text{e}^- \rightarrow \text{H}_2 + 2\text{OH}^-$	$2\text{H}^+ + 2\text{e}^- \rightarrow \text{H}_2$	$\text{H}_2\text{O} + 2\text{e}^- \rightarrow \text{H}_2 + \text{O}^{2-}$
Anode reaction	$2\text{OH}^- \rightarrow \text{H}_2\text{O} + \frac{1}{2}\text{O}_2 + 2\text{e}^-$	$\text{H}_2\text{O} \rightarrow 2\text{H}^+ + \frac{1}{2}\text{O}_2 + 2\text{e}^-$	$\text{O}^{2-} \rightarrow \frac{1}{2}\text{O}_2 + 2\text{e}^-$
Efficiency (%)	59-70	65-82	Up to 100
Hydrogen purity (%)	>99.8	99.999	-
Temperature(°C)	20-80	20-200	500-1000
Current density (A/cm²)	0.2-0.4	0.6-2.0	0.3-2.0
Voltage (V)	1.8-2.4	1.8-2.2	0.7-1.5
Stack energy consumption (kWh/Nm³)	4.2-5.9	4.2-5.5	>3
Capital cost (USD/kW)	880-1650	1540-2550	>2000
Lifetime of stack (kh)	60-120	60-100	8-20
Cold start time (min)	>15	<15	-
Technology readiness level	TRL-9	TRL-7	TRL-5
Technology maturity	Commercial	Near commercial	Demonstration
Advantages	Low capital cost compared with PEMWE and SOEC, relatively stable and mature technology	Compact design, fast dynamic response, high gas purity	High electrolysis efficiency, low energy requirements
Disadvantages	Long starting time, slow dynamic response, highly corrosive	Dependence on precious metal catalysts, high cost	Rapid material degradation, short running life, high manufacturing costs
Challenges	Improve dynamic performance, electrolysis efficiency, reliability, safety	Reduce noble-metal utilization	Electrode microstructure changes

2.2 Literature survey

The primary challenge in the socio-economic development for the future lies in the substitution of fossil fuels. Green hydrogen serves as the most promising solution towards solving this

challenge making it the most credible energy carrier. In particular, hydrogen generation through the electrocatalytic water splitting based on green electricity has significantly fewer CO₂ footprints. The technologies used commercially for green hydrogen production are alkaline, proton exchange membrane and solid oxide electrolysis depending on the electrolyte used. Out of these, alkaline water electrolysis stands out as the most mature, and widely applicable technology in industries for green hydrogen production.

Regardless of the alkaline water electrolysis widespread use in industry, its properties are still being studied due of the complex transport phenomena associated with multiphase flow [18]. A lot of work has gone into modeling, characterizing, and optimizing the operation of AWE. For this, Ulleberg [38] introduced one of the most commonly used models in which a computational model was built for an advanced alkaline electrolyzer that integrates fundamental thermodynamics, heat transfer, empirical electrochemical relationships and the model was validated to show its capability to accurately predict the behavior of the system. Several other models with varying assumptions and simplifications were reported in the literature [26], [39], [40], where the electric and thermal aspects in the spatial domain were ignored by these multi-physics models and considered AWE as a lumped-parameter system. Additionally, the lumped-parameter model fails to account for the bubble curtain generated in the electrolysis cell and the turbulence resulting from gas and liquid phase interactions.

Under these conditions, computational fluid dynamics (CFD) simulations emerge as a powerful computational tool for improving flow distribution, reducing energy consumption, and model complex electrochemical processes of alkaline water electrolysis [41]. Computational fluid dynamics (CFD) is an important tool for analyzing the simultaneous complex interactions that exist between heat transfer, electrochemistry, and fluid flow in AWE cells. The understanding of these complex interaction is essential to improve the behavior, design, and efficiency of the AWE cells for hydrogen production.

The multi-phase behavior of AWE cell was simulated in [42], to study the influence of different operating conditions on the behavior of cell, and the CFD model's accuracy is determined by validating it with experimental results. In [43], the hydrodynamics of multiphase flows, impact of turbulent dispersion forces on the alkaline electrolyzer were studied and the importance of accurate predictions of the bubble curtain spreading along with the role of interphase forces in the accuracy of the CFD model were highlighted. A CFD model was built using in literature [44], that simultaneously analyses the gas-liquid distribution and polarization curves to model

the behavior of the AWE cell, afterwards the operating parameters were optimized for maximum hydrogen production using a lumped model. Several other two-phase flow CFD models were studied for alkaline water electrolysis in literature [45], [46].

Machine learning is a subgroup of artificial intelligence (AI) that helps teaching computers to learn from the past examples, data, and patterns in order to make predictions based on their training [47]. In the energy sector, machine learning applications has grown significantly in the last several years. ML techniques like artificial neural networks (ANN) are employed to make predictions of the energy demand, consumption patterns and optimize power grid operations [48], [49]. Also, artificial neural networks play a critical role in integrating renewable energy sources by predicting the solar or wind power output, and help optimize energy generation and storage systems, hence promoting the effective use of renewable resources [50], [51].

An ANN approach is employed in a simulation model in [52], to predict the efficiency of hydrogen production through gasification, predicting the impact of operating parameters and biomass properties. In literature [53], modeling and optimization of a hydrogen plant is performed using ANN, and insights into finding the optimum number of neurons in the hidden layer were provided. Optimization of an AWE cell through an integrated approach of CFD modeling and ANN is performed in [54], in order to predict the performance of the cell under different operating conditions and find the optimal conditions. Previous literature shows that hydrogen production using artificial neural networks (ANN) were mostly focused on methods consisting of hydrocarbons, which leads us to a research gap in hydrogen production, particularly through water electrolysis.

This research presents a novel technique to predict the performance of a 2D alkaline water electrolysis cell under different operating values of temperature, KOH electrolyte conductivity and the distance between electrode and diaphragm, using an integrated approach of CFD and ANN. The integrated approach improves the efficiency and performance of AWE to gain a complete understanding of the cell's behavior. The purpose of this study is to optimize the AWE cell for faster predictions and better understanding, while significantly reducing the computational resources.

CHAPTER 3: RESEARCH METHODOLOGY

3.1 Overview of Alkaline Water Electrolysis

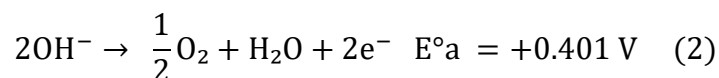
The modeling of alkaline water electrolysis started in 1990s, despite having a long history. In Alkaline water electrolysis, water splitting technique is employed for hydrogen production, in which electricity is passed between two electrodes to split water molecules into hydrogen and oxygen. Hydrogen produced by electrolysis is considered as a clean fuel and is used in fuel cells, transportation, and other applications [1]. AWE is the most mature technology among others, and has been in use for hydrogen production in industries for several decades now [19].

The electrochemical process is carried out in an electrochemical cell which consists of two electrodes i.e., cathode and anode separated by a diaphragm and bipolar plates. The diaphragm is a thin, porous material that separates the anode and cathode and prevents the mixing of gases produced during the electrolysis process. KOH electrolyte is introduced into the electrolyzer from the bottom as shown in figure 1 which is then distributed to the two electrodes via diaphragm. The electrochemical reactions start taking place as soon a direct current is applied between the electrodes.

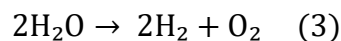
At cathode, reduction of water molecules takes place to produce hydrogen (H₂) and OH⁻ ions.



These OH⁻ ions then move to the anode side and are oxidized to produce oxygen (O₂) and water (H₂O) molecules, thus maintaining the charge balance.



The overall reaction for an alkaline water electrolysis cell is:



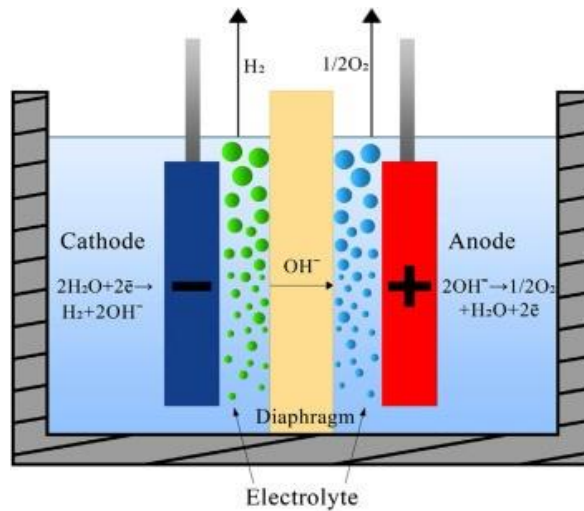


Figure 3.1: Alkaline water electrolysis. [55]

Hydrogen produced from hydroelectric power through alkaline water electrolysis is renewable in nature, and that is why it is called green hydrogen. The electrolyzers however are of two types based on their construction and design i.e. monopolar and bipolar as shown in figure 2. Bipolar structure of electrolyzers is when the electrodes of cells in a stack are connected in series, offering high efficiency and compact structure because the electrodes of each cell are connected end to end. Similarly, when the electrodes of these cells are connected in parallel, it is known as a monopolar structure. This setup offers a series of advantages such as lasting durability and simple design, but the electrodes in the stack are separated, creating a complex external electric circuit for connection, which causes power loss and use of extra material [38].

No matter how the electrolyzer is set up, the major disadvantage of the alkaline water electrolysis cells is the formation of bubbles at the two electrodes [24]. These formed bubbles then mess with the properties of the KOH electrolyte. They alter its ability to conduct ions, which in turn increases the cell's overpotentials and the overall cost of operating cell. Also, if the mass transport is not properly balanced, there is a chance that the H₂ and O₂ bubbles will start intermixing. The intermixing is not just a safety concern during operation, but also affects the purity of the gases produced [56], [57].

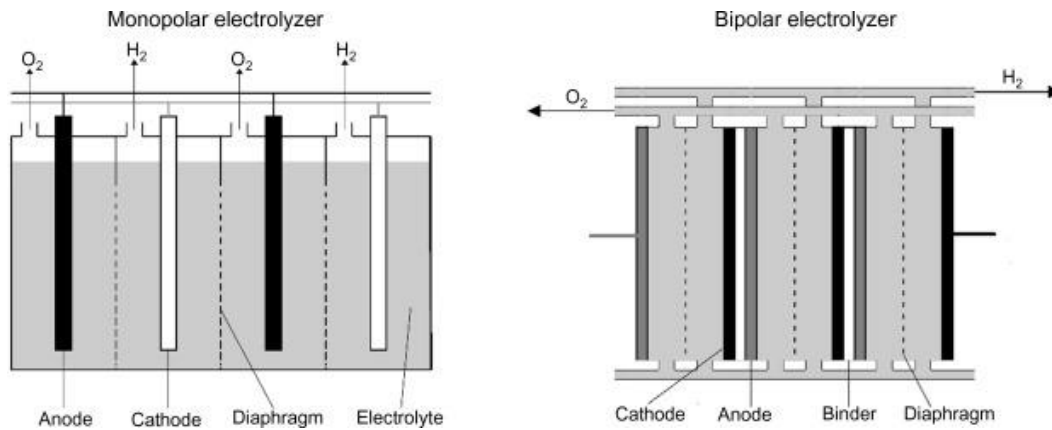


Figure 3.2: Alkaline water electrolyzer structure: (a) monopolar and (b) bipolar [58].

3.2 Process Description and Model Development

The electrolysis cell is the main component, but just a part of the whole system of AWE. Some outer components are also required to efficiently produce pure hydrogen. In figure 3, a schematic diagram of a single alkaline electrolysis cell is shown providing general overview of the outer components and working of an AWE system [44]. At first, the electrolyte solution is contained in a reservoir, from where it is sent to a heater to heat the electrolyte solution up to a required temperature of around 80-90°C. The electrolyte solution then filtered before entering the electrolyzer cell to remove the impurities. The electrolyzer cell is the main component of this system and it consists of two channels, one for hydrogen gas and the other for oxygen. These two gas channels are separated by a diaphragm and connected to a power source that provides the electric current to drive the electrochemical reactions that involves splitting of the solution into oxygen and hydrogen. The electrolyte and gas mixture are then separated, and the KOH electrolyte is recycled and used again within the system. Each component is important in this system for the efficient hydrogen production. Figure 4 shows the simplified representation of the basic operating principle and the energy flow in the AWE system.

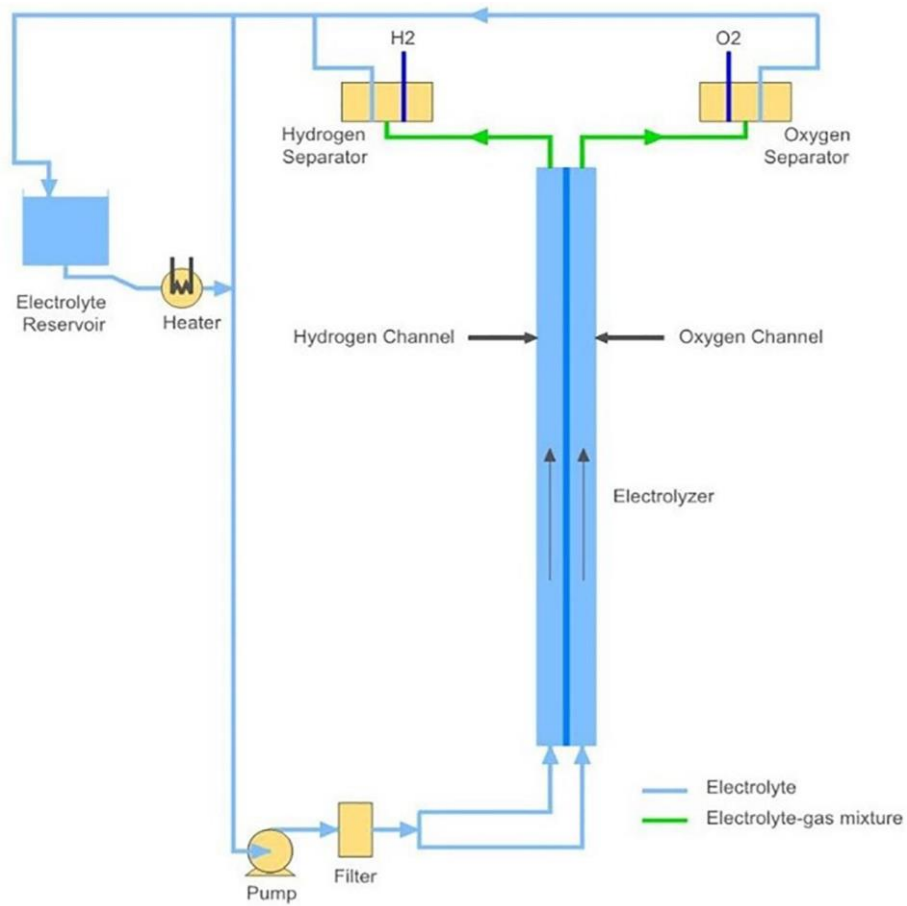


Figure 3.3: A single AWE cell with its other components [44].

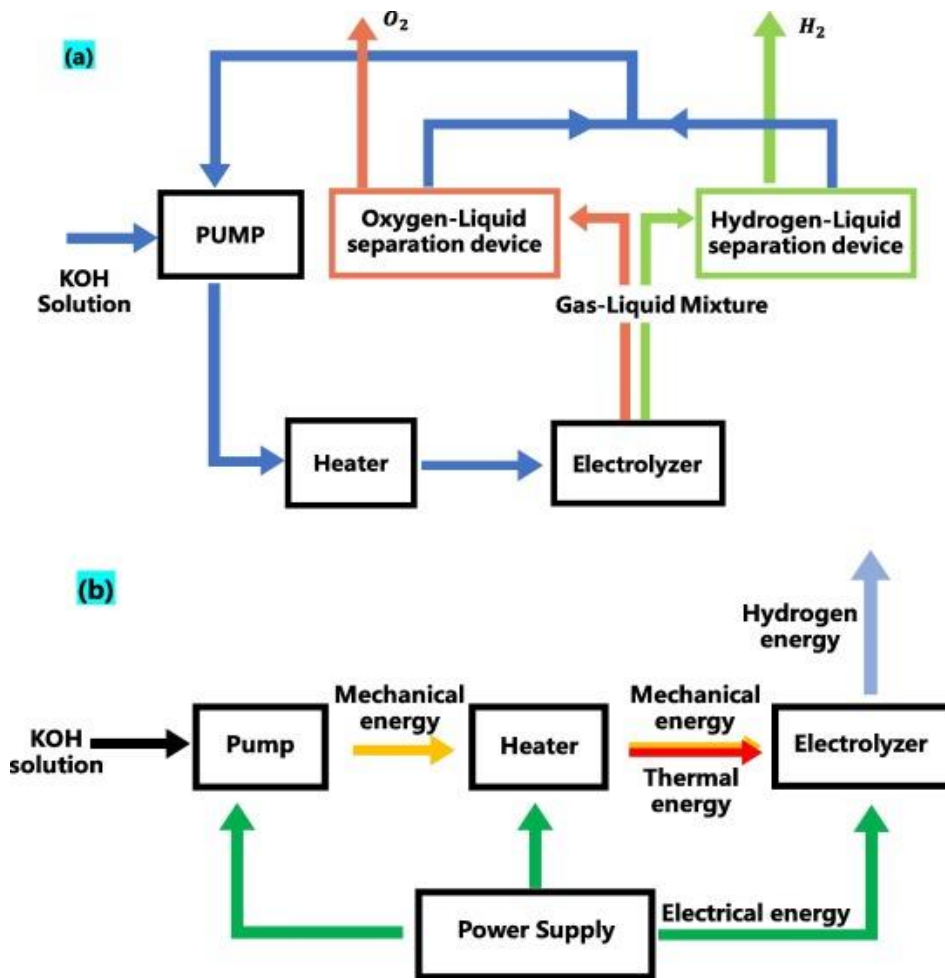


Figure 3.4: A simplified representation of the AWE system (a) basic operation (b) Energy flow in the AWE [59].

3.3 Proposed Methodology

The methodology of this research is proposed in Figure 5. The research starts with simulating a 2D alkaline water electrolysis cell using computational fluid dynamics. The computed results were then post processed and a parametric sweep was applied on a range of values of temperature, current density and electrolyte weight concentrations of KOH. The generated datasets through this sweep were then exported to MATLAB. Using a MATLAB code, the datasets were divided into three categories such as training, testing and validation datasets. An artificial neural network was trained using the NN toolbox and the ANN's performance was analyzed through regression plots. Lastly, the ANN results were validated with CFD output results.

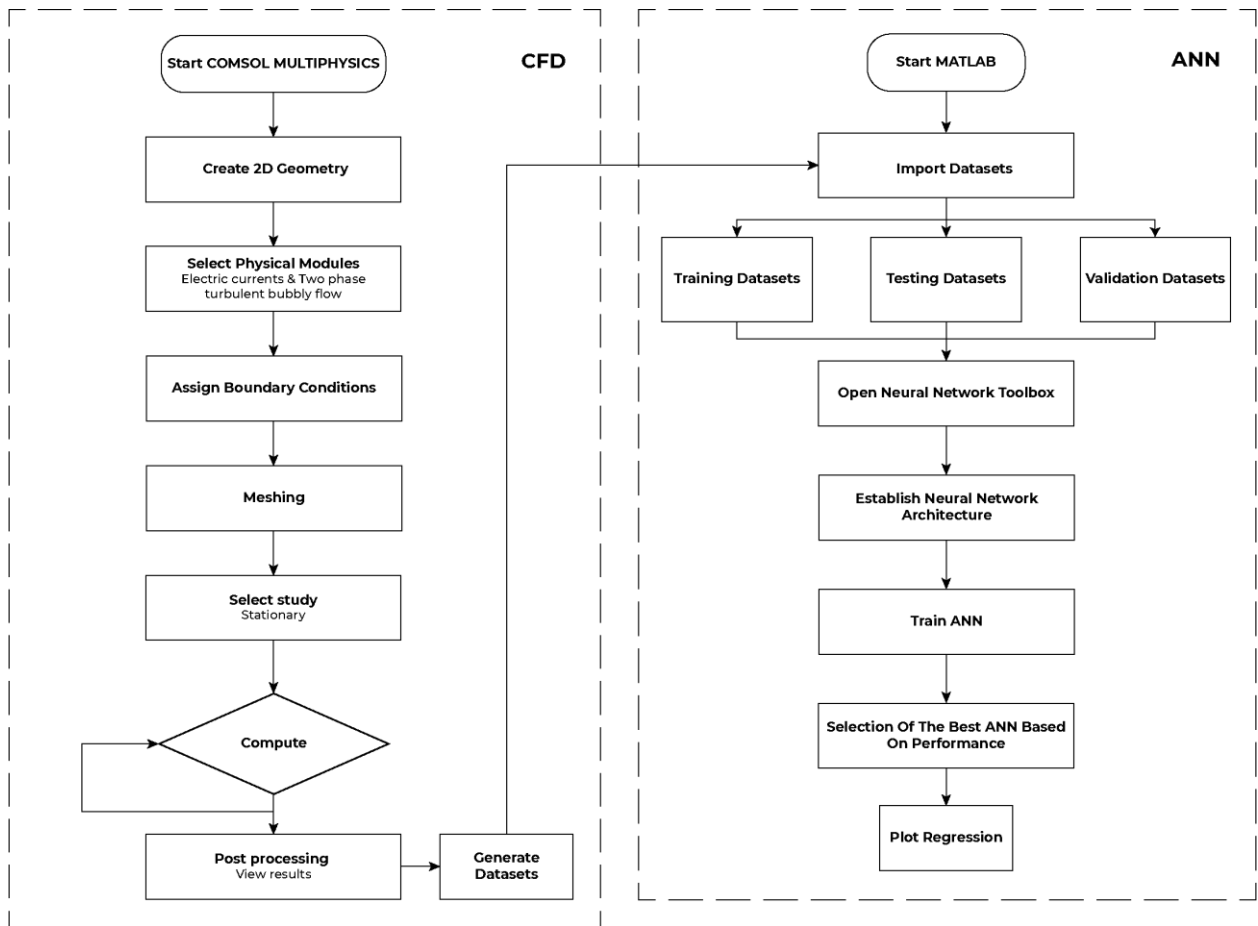


Figure 3.5: Flowchart of the proposed methodology.

CHAPTER 4: CFD MODELING OF ALKALINE WATER ELECTROLYSIS AND DATA GENERATION

4.1 AWE CFD Modeling Setup and Parameters

Alkaline water electrolysis is an electrochemical process in which water molecules are decomposed into hydrogen and oxygen by the application of electric current directly passed between the two electrodes i.e. cathode and anode. These two electrodes are separated by a thin diaphragm, which is made up of a porous material that prevents the mixing of gases produced during the process [55]. Although the process of AWE is conceptually simple, it involves several complex fluid dynamics, thermodynamics, and electrochemical phenomena. To study these complex phenomena simultaneously, computational fluid dynamics (CFD) simulations are utilized. CFD simulations have proved to be an important tool in solving problems that are expensive experimentally and time-consuming. It can help us refine and innovate new techniques to enhance the efficiency and develop new models that are iteratively simpler to the more complex numerical analyses. CFD simulations emerge as a powerful computational tool for improving flow distribution, reducing energy consumption, and model simultaneous complex interactions that exist between heat transfer, electrochemistry, and fluid flow in AWE cells [43]. The understanding of these complex interaction is essential to improve the behavior, design, and efficiency of the AWE cells for hydrogen production.

To improve the performance and understand behavior of the fluids and gases in the AWE cell, electrochemical and fluid dynamic response of the cell is captured accurately for maximum efficiency. The two-phase flow adds complexity to the AWE model, proving a more accurate and comprehensive representation of AWE process. Also, the complex electrochemical, mass transfer and fluid dynamic phenomena within the AWE cell are more accurately analyzed for improved performance and efficiency to produce hydrogen.

4.1.1 Geometry and Discretization

The AWE CFD model is built on COMSOL MULTIPHYSICS software. A simple 2D geometry is preferred for this model, since most lab scale AWE cells are rectangular [42]. The geometry consists of two electrodes i.e. cathode and anode, and a diaphragm that separates them. The dimensions of cathode and anode are the same, the width

of 1.5mm, 4mm and 10mm is used. For diaphragm, a thin rectangle of 0.5mm width is used. The height or length of each electrode and diaphragm is set as 33mm. The geometric parameters of the AWE cell are given in Table 2. A two-phase model is used for the complex modeling of AWE cell with these geometric parameters. However, if complex AWE system and more flows channels are associated with the model, then 3D geometry are employed for AWE cells [60]. The AWE cell's geometry was meshed using the quadrilateral and triangular elements. Extra fine layers were incorporated at the electrode boundaries and the boundaries between diaphragm and the electrodes. Additional details regarding meshing can be found in Table 3.

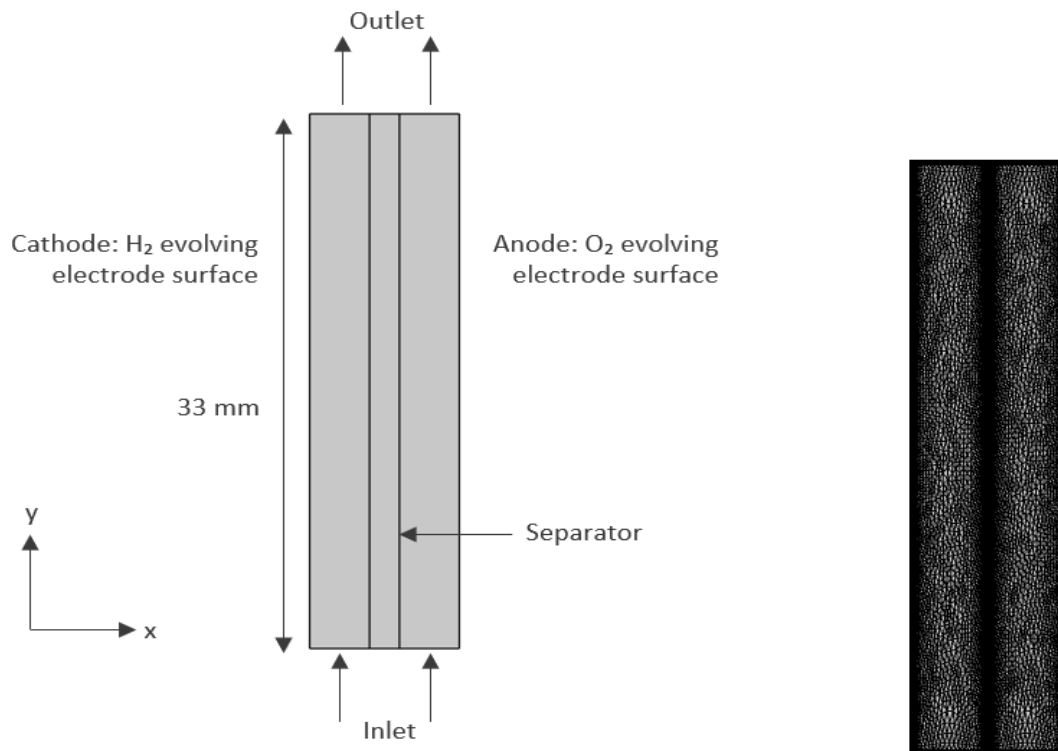


Figure 4.1: Mesh configuration of the cell.

Table 4.1: Geometric parameters

Parameters	Value	Units
Cathode compartment width	1.5, 4, 10	mm
Diaphragm width	0.5	mm
Anode compartment width	1.5, 4, 10	mm
Cell width	3.5, 8.5, 20.5	mm
Electrodes length	33	mm
Diaphragm length	33	mm

Table 4.2: Mesh statistics

Mesh Statistics	Values
Number of Elements	13240
Triangular Elements	10750
Quadrilateral Elements	2490
Mesh Vertices	8059
Edge Elements	634
Vertex Elements	12

4.2 Physical Modules and Governing Equations for CFD Simulations

Polarization curves are generated at different operating parameters to evaluate the AWE cell's performance. In this work, a 2D alkaline water electrolysis model was simulated using two modules, electric current and two-phase turbulent bubbly flow ($k - \varepsilon$ model). The electrochemical reactions occurring in AWE cell are studied using electric current physical module and also the relation between voltage and current density is simulated. While the interactions between the two phase i.e. gas-liquid phase and the turbulence in the flow channels due to the formation of bubbles is studied using the bubbly flow module.

In this work, various parameters were used, their values are provided in table 4.

Table 4.3: Model parameters for two-dimensional (2D) AWE cell [42], [44], [61]–[63]

Parameter	Value	Unit
Temperature	303.15 - 343.15	K
Pressure	1	bar
Current density	0 - 3500	A.m ⁻²
Exchange current density (cathode)	21.9– 74.8	A.m ⁻²
Exchange current density (anode)	1.05 – 9.1	A.m ⁻²
Faraday constant	96485	C
Ideal gas constant	8.314	J. K ⁻¹ .mol ⁻¹
Electrode-diaphragm distance	1.5 - 10	mm
Molecular weight (hydrogen)	2	g.mol ⁻¹
Molecular weight (oxygen)	32	g.mol ⁻¹
Electrolyte velocity	0.032	m.s ⁻¹
KOH concentration	22 - 32	wt%
Diaphragm relative permittivity	77.2	-
Diaphragm porosity	0.55	-
Diaphragm tortuosity	1.89	-

4.2.1 Electric currents

The current conservation problem is solved by solving the equations of the electric current physics. The cell voltage and current density are the important parameters calculated using this physical module. To solve this, equation (4) is employed.

$$\nabla \vec{J} = Q_j = -\nabla \cdot \left[\sigma(\nabla U) - \frac{\partial \vec{D}}{\partial t} - \vec{J}_e \right] \cdot d = Q_j \cdot d \quad (4)$$

where σ represents the electrical conductivity (S/m), \vec{J}_e is the current density (A/m), Q_j is the current source, d is the surface thickness. And $\frac{\partial \vec{D}}{\partial t}$ is the electric displacement.

The electrical conductivity (σ) of the electrolyte was calculated to solve the current conservation problem in equation (4), it can be calculated by equation (5) [64];

$$\sigma_0 = -204.1 \cdot c - 0.28 \cdot c^2 + 0.5332 \cdot (c \cdot T) + 20720 \cdot \frac{c}{T} + 0.1043 \cdot c - 0.00003 \cdot (c^2 \cdot T^2) \quad (5)$$

where T is the temperature and c is the concentration of electrolyte (KOH).

Bruggman equation (6) helps us calculate the overall conductivity (σ_e), it relates the conductivity of electrolyte (σ_0) with the volume gas fraction (Φ_g) at each current density for both the cathode and anode [65].

$$\sigma_e = \sigma_0 \cdot (1 - \Phi_g)^{1.5} \quad (6)$$

where, Φ_g was calculated by the turbulent physics.

We can calculate diaphragm's conductivity by equation (7) [61];

$$\sigma_m = \sigma_0 \cdot \frac{\epsilon_m}{\tau_m} \quad (7)$$

where, ϵ_m is porosity and τ_m is tortuosity.

The electrochemical reactions occurring within the AWE cell were initiated by applying a minimum voltage of 1.23V at 1 atm and 298K known as the reversible voltage (U_{rev}).

The electric current is supplied to the AWE cell which triggers certain losses, due to which some electric energy is lost as heat. This causes the demand of more energy than what is thermodynamically required for the reaction to occur. This extra energy is the overpotentials or irreversibility which is higher than the initial voltage of 1.23V.

The AWE cell's total potential is provided by equation (8);

$$U = U_{rev} + \sum n \quad (8)$$

The overpotentials usually depend on the operation conditions and the design of the cell. We calculate the reversible and activation overpotentials by equations (9) and (10) respectively to study their effects in the polarization curve [2], [66].

$$U_{\text{rev}} = 1.5184 - 1.5421 \times 10^{-3}T + 9.523 \times 10^{-5}T \ln T + 9.84 \times 10^{-8}T^2 \quad (9)$$

$$U_{\text{act}} = 2.3 \frac{RT}{\alpha F} \log\left(\frac{i}{i_0}\right) \quad (10)$$

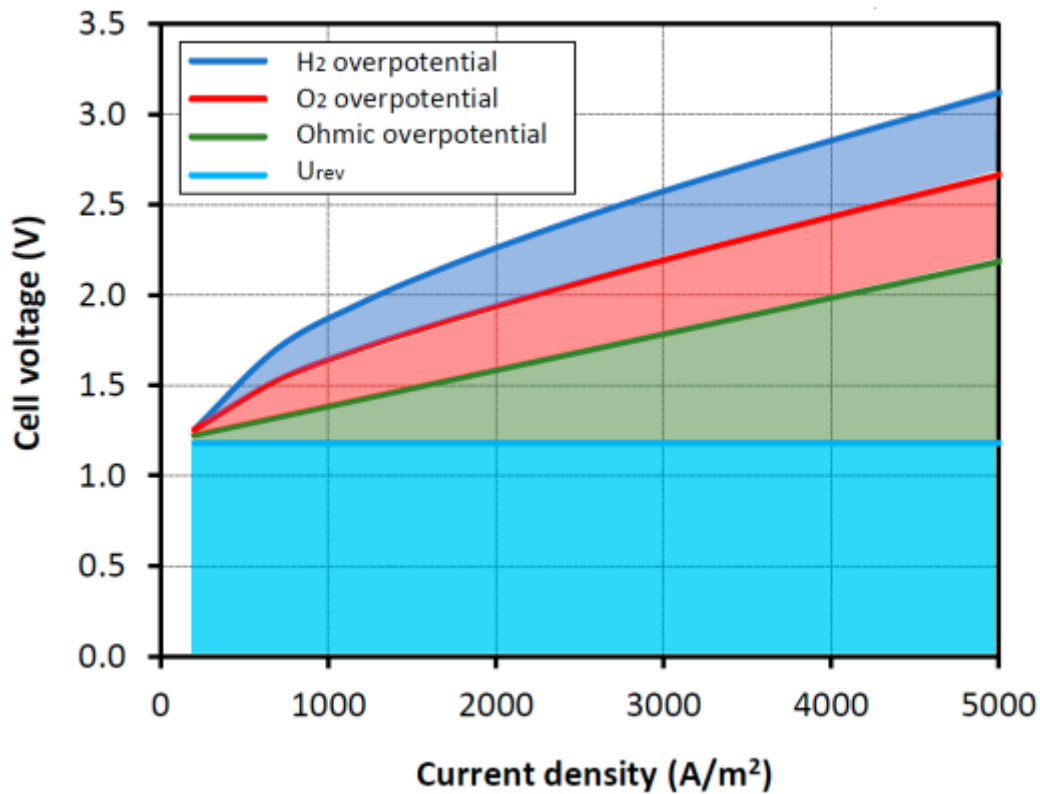


Figure 4.2: Compositions of various AWE cell potentials [42].

4.2.2 Two-phase turbulent bubbly flow ($k - \epsilon$ model)

The interactions between the gas-liquid phase and the turbulence within the AWE cell is modeled using this module. Also, the volume gas fraction occupied by each phase is determined. Euler-Euler model is utilized by the turbulent flow physics to explain the two-

phase flow. The equation (11) and (12) are the momentum and continuity equation, respectively.

$$\begin{aligned} \Phi_1 \cdot \rho_1 \cdot \frac{\partial \vec{u}_1}{\partial t} + \Phi_1 \cdot \rho_1 \cdot (\vec{u}_1 \cdot \nabla) \vec{u}_1 = -\nabla p + \nabla \cdot \left[\Phi_1 \cdot (\psi_1 + \psi_T) \cdot \left(\nabla \vec{u}_1 + \nabla \vec{u}_1^T - \frac{2}{3} \cdot (\nabla \vec{u}_1) \cdot \vec{I} \right) \right] \\ + \Phi_1 \cdot \rho_1 \cdot \vec{g} + \vec{F} \quad (11) \end{aligned}$$

$$\frac{\partial}{\partial t} (\Phi_1 \cdot \rho_1 + \Phi_g \cdot \rho_g) + \nabla \cdot (\Phi_1 \cdot \rho_1 \cdot \vec{u}_1 + \Phi_g \cdot \rho_g \cdot \vec{u}_g) = 0 \quad (12)$$

The transport of volume gas fraction is given by equation (13);

$$\frac{\partial \Phi_g \cdot \rho_g}{\partial t} + \nabla \cdot (\Phi_g \cdot \rho_g \cdot \vec{u}_g) = -\dot{m}_{gl} \quad (13)$$

Where, \dot{m}_{gl} represents the rate of mass transfer from the gas to liquid phase. Hydrogen and oxygen gases produced in the gas chambers are calculated by the Faraday equation.

$$\dot{m}_{H_2} = \frac{M_{H_2}}{2 \cdot F} \cdot i \quad (14)$$

$$\dot{m}_{O_2} = \frac{M_{O_2}}{4 \cdot F} \cdot i \quad (15)$$

Here, one other model is also utilized which is the $(k - \varepsilon)$ turbulence model. This model solves two additional transport equations (17) and (18).

$$\psi_T = \rho_1 \cdot C_\mu \cdot \frac{k^2}{\varepsilon} \quad (16)$$

$$\rho_1 \cdot \frac{\partial k}{\partial t} - \nabla \cdot \left[\left(\psi + \frac{\psi_T}{\Phi_k} \right) \nabla k \right] + \rho_1 \cdot \vec{u}_1 \cdot \nabla k = \frac{1}{2} \psi_T \cdot (\nabla \vec{u}_1 + (\nabla \vec{u}_1)^T)^2 - \rho_1 \cdot \varepsilon + S_k \quad (17)$$

$$\begin{aligned} \rho_1 \cdot \frac{\partial \varepsilon}{\partial t} - \nabla \cdot \left[\left(\psi + \frac{\psi_T}{\Phi_\varepsilon} \right) \nabla \varepsilon \right] + \rho_1 \cdot \vec{u}_1 \cdot \nabla \varepsilon \\ = \frac{1}{2} C_{\varepsilon 1} \cdot \frac{\varepsilon}{k} \cdot \psi_T \cdot (\nabla \vec{u}_1 + (\nabla \vec{u}_1)^T)^2 - \rho_1 \cdot C_{\varepsilon 2} \cdot \frac{\varepsilon^2}{k} + \frac{\varepsilon}{k} C_\varepsilon \cdot S_k \end{aligned} \quad (18)$$

The above equations include constants such as C_μ , C_ε , Φ_ε , and Φ_k . S_k represents the turbulence induced by bubbles. Also, \vec{u}_{slip} is the relative velocity between the two phases, and \vec{u}_{drift} is an additional term within the turbulence model.

$$\vec{u}_g = \vec{u}_l + \vec{u}_{\text{slip}} + \vec{u}_{\text{drift}} \quad (19)$$

Exchange current density at anode and cathode are calculated by the equation (20) and (21), respectively [44].

$$i_{0,a} = 10^{\left(-\frac{2413.7}{T} + 8.0219 \right)} \quad (20)$$

$$i_{0,c} = 10^{\left(-\frac{1388.6}{T} + 5.932 \right)} \quad (21)$$

4.3 Data Generation for ANN model

The performance of the 2D CFD model of alkaline water electrolysis is determined by the electrochemical response of the cell. The electrochemical response is obtained through polarization curves under different values of temperature, KOH conductivity and electrode-diaphragm distance. The model results are validated with the experimental ones using the generated polarization curves at different values of the operating parameters. Datasets of the 2D AWE CFD model was generated by applying a parametric sweep over a range of values of temperature, current density, and KOH electrolyte weight concentration.

A large dataset was created and exported from COMSOL MULTIPHYSICS to Excel for each operating parameter. Then the datasets were exported to MATLAB and divided into three different categories i.e., 70% of the exported data for training, 20% for testing and the rest 10% for validation, using a code generated on MATLAB. In summary, we generated datasets by

linking COMSOL with Excel, and then integrated Excel with MATLAB for the division of data into training, testing and validation datasets. Finally, an artificial neural network (ANN) model was trained and validated using neural network toolbox in MATLAB software [35], [44].

4.4 ANN Model Training and Validation

The process of ANN modeling includes three stages: selection of the model, training, and validation. The Levenberg-Marquardt training algorithm is used to train the ANN model. The dataset was divided into three different categories i.e., 70% of the samples for training, 20% for testing and 10% for validation. The ANN model is trained by providing the datasets generated from the CFD model which includes different input values of AWE cell temperature, current density, and the KOH electrolyte weight concentrations. The ANN model is training using these datasets in order for it to learn the complex patterns and relationships between the input parameters and the target variables using the Levenberg-Marquardt training algorithm. The validation of the ANN model is an important step to ensure its predictive accuracy and is computed using metrics like mean-squared error (MSE), root-mean-squared error (RMSE) and the correlation coefficient (R). The model is trained and validated rigorously to enhance the prediction capability of the neural networks for the AWE cell's performance. MSE, RMSE and R^2 were calculated using the following equations respectively [67];

$$\text{MSE} = \frac{1}{n} \sum_{i=1}^n (Y_{i,\text{pred}} - Y_{i,\text{CFD}})^2 \quad (22)$$

$$\text{RMSE} = \sqrt{\frac{1}{n} \sum_{i=1}^n (Y_{i,\text{pred}} - Y_{i,\text{CFD}})^2} \quad (23)$$

$$R^2 = 1 - \frac{\sum_{i=1}^n (Y_{i,\text{pred}} - Y_{i,\text{CFD}})}{\sum_{i=1}^n (Y_{i,\text{pred}} - Y_{\text{avg}})} \quad (24)$$

where, n is the total number of samples, $Y_{i,\text{pred}}$ is the predicted ANN values, $Y_{i,\text{CFD}}$ is the CFD output values and Y_{avg} is the average values.

CHAPTER 5: ARTIFICIAL INTELLIGENCE MODEL ARCHITECTURE

5.1 Introduction to Artificial Intelligence and Machine Learning

In recent years, artificial intelligence (AI) has captured widespread attention within the scientific community. A lot of research has been done to explore AI and ML. AI techniques like machine learning and deep learning are employed to automate the intelligent tasks typically carried out by humans [68]. In ML, systems autonomously acquire knowledge without much programming [69]. The focus lies in making the computer programs capable of accessing data and self-learning. This process begins by accessing the data, learning the data patterns in order to enhance the ability of decision-making and to enable systems to learn without any human involvement. The ML algorithms are divided into supervised, unsupervised and reinforcement learning.

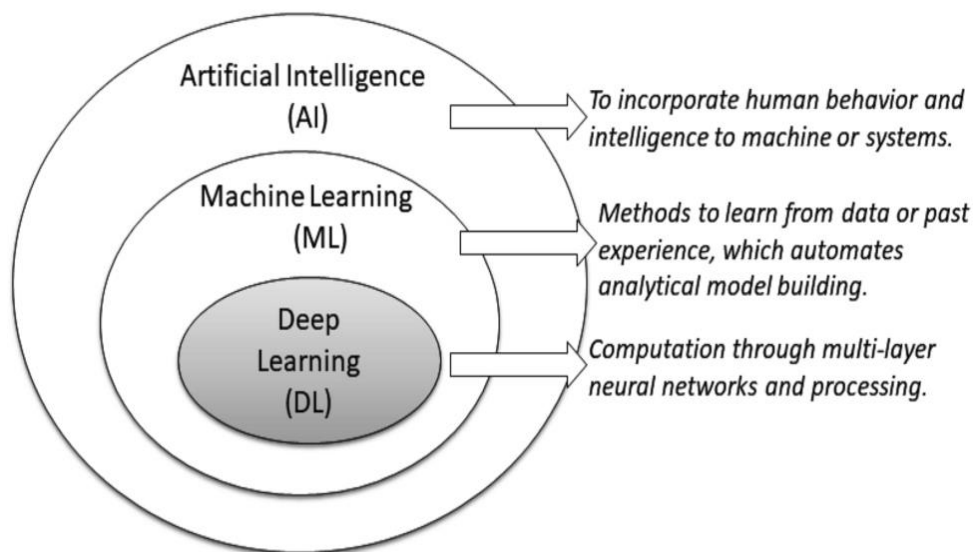


Figure 5.1: Difference between AI, ML and DL [70].

5.2 Overview of Artificial Neural Networks

Artificial neural network (ANN) is an AI and machine learning technique used to solve complex problems and models. The structure and function of the ANN models were inspired by the human brain as they are designed to copy the behavior of biological neural networks. Recently, the use of ANN has increased as it has become more useful for applications like regression, decision making, pattern recognition etc. In ANNs, large number of nodes are interconnected and work simultaneously to learn the patterns and analyze the input data to make better predictions.

The ANN's ability to learn complex patterns and relationships from large input data, also adjusting the weights and biases parameters for better predictions makes them a novel and highly efficient tool in problem solving and other machine learning applications. ANN also has the advantage to learn from both labelled and unlabelled data, which makes them a compatible tool for supervised and unsupervised learning applications like classification, clustering, and regression. They are also useful in application such as speech and image recognitions, pattern recognition and signal processing.

This makes the ANN an effective and reliable tool for making effective predictions based on the relations, examples, and patterns within the provided data, and have applications in many fields that include chemical and process engineering, robotics, medicine, finance, and many more real-world complex problems [75]. An ANN model is utilized in this research and the AWE cell's performance in terms of current density and cell's voltage values were predicted. The datasets provided to train the ANN model were generated from a CFD 2D model of AWE cell using COMSOL MULTIPHYSICS.

5.3 Architecture of the ANN Model

The ANN's architecture usually involves its structure in which large number of nodes are interconnected and work simultaneously to learn the patterns and analyze the input data to make better predictions at the output. As shown in figure 9, the main layers in ANN architecture include:

5.3.1 Input Layer

ANN consists of three main layers: input, hidden and output layer. The first layer in the ANN's structure is the input layer. The function of which is to receive information and data from external environments. In this layer, each neuron signifies an input variable or feature. It is the entry point of the data and transfers the data to the other layers in the ANN structure.

5.3.2 Hidden Layers

There can exist one or more hidden layers in between the input and output layers. Depending on the complexity of the problem and training data, the number of neurons present in each layer is determined. Most of the data processing takes place in hidden layers. The neurons present in these layers play an important role in analyzing and learning data, information, and the complex patterns within the data.

5.3.3 Output Layer

The final layer in the ANN structure is the output layer and the neurons present in the layer are liable for generating the final decisions and predictions based on the data processed. The number of neurons that exist in this layer usually depends on the complexity of the problem and the output data obtained is a result of the data processed in the preceding layers.

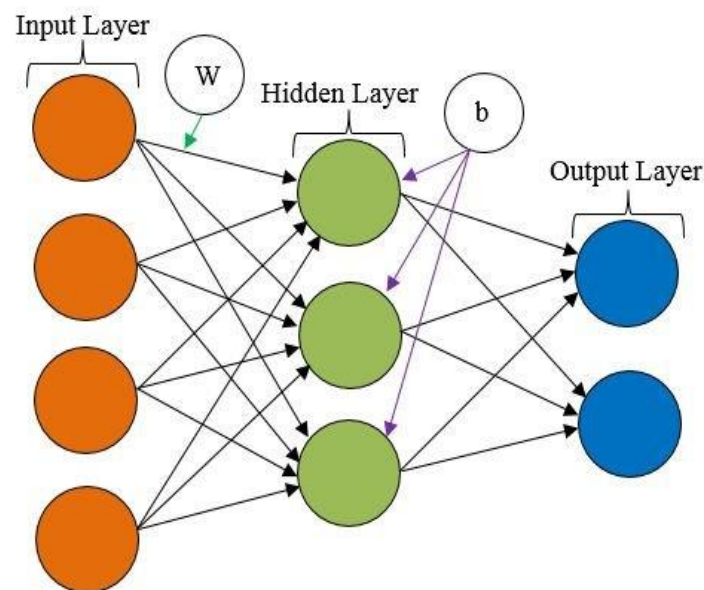


Figure 5.2: Architecture of multiple inputs and outputs ANN

5.4 ANN Components

The function of the ANN was inspired by the working of human brain and is structured to replicate the behavior of the biological neural networks. In ANN, interconnected nodes are present that work simultaneously to analyze the data and learn pattern based on the input data and make better decisions. The main component of ANN include:

5.4.1 *Neurons*

The main processing units of an ANN is neurons. Neurons are also known as nodes and receive input for processing and based on the training data generates an output signal for the other layer which is transmitted with the of neurons. Each neuron in the layer applies a weighted sum of the inputs, includes bias term, and then applies activation function in order to generate an output. These neurons are interconnected and are present in each layer i.e. input, output and hidden layers through weighted connections.

5.4.2 *Weights*

The strength of the neuron's connections in each layer of the neural network are represented by the parameters called weights. Every connection that exists between neurons has some associated weight that will decide the impact of the input signal on the output of the neuron. The values of weights at the start are set randomly and then updated during the training interactively using some algorithms and weights are adjusted to reduce the prediction error.

5.4.3 *Biases*

Biases are the added parameters in neurons, which enable ANN to model complex patterns and relationships and make predictions on the basis of data provided.

Also, each neuron has a bias term that is added to the weighted sum of inputs before the activation function is applied. In particular, biases offer good flexibility in modeling and enables ANN to learn and represent patterns which may not be captured by the input data alone.

5.4.4 *Activation Function*

An activation function determines the neuron's output for a specific input. It introduces nonlinearity to the network, which lets the ANN analyze and model complex relationships and make accurate decisions or predictions.

These components work together and allow ANNs to learn from data and make accurate predictions.

CHAPTER 6: RESULTS AND DISCUSSION

6.1 CFD Modeling and Validation of AWE cell

A 2D AWE cell was simulated and different responses such as electrochemical and fluid dynamic response were analyzed using COMSOL MULTIPHYSICS 6.1. The behavior of the cell was analyzed using the two physical modules, and the distribution of current across the cell, efficiency of the electrochemical reactions, and the relation between voltage and current density were also simulated. Also, the gas-liquid phase interactions, turbulence created due to the formation of bubbles in the gas domains were analyzed through the fluid dynamic response of the cell. By simulating all these phenomena simultaneously, the performance of the AWE cell was enhanced, and more hydrogen can be produced using the CFD model.

The CFD model results were validated with the experimental data to ensure the accuracy of the AWE model using polarization curves under different operating conditions. Then, datasets were generated by applying a parametric sweep over a range of values of temperature, current density, and KOH electrolyte weight concentration. The datasets were exported from COMSOL to Excel for each operating parameter. Later, they were exported to MATLAB and divided into three different types by using a MATLAB code. 70% of the datasets were used for training, 20% for testing and 10% for validation of the ANN model. At the end, the ANN model results were validated against COMSOL output data.

6.2 Influence of operating parameters on the CFD model

The electrochemical response simulated with the help of polarization curves. The polarizations curves generated from CFD simulations were then validated against the experimental data and minimal error was obtained.

6.2.1 *Influence of Temperature*

At different temperatures, the polarization curves were generated in order to simulate the influence of temperature on the performance of the cell. CFD simulations at different temperatures, 32 wt% KOH electrolyte weight concentration, 10mm electrode-diaphragm distance and 0.033 m/sec electrolyte velocity were performed. The results generated by the

CFD model using these operating conditions were then compared with the experimental data to ensure its accuracy. Figure 10 shows the model results align closely with the experimental data. Few observations were made by analyzing the polarization curve, that as the temperature increase the cell voltage decreases. This is because, when temperature rises from 30°C-70°C, it speeds up the reaction kinetics, leading to a decrease in the reversible voltage and which reduces the energy required. This increases the efficiency of the AWE cell.

So, when the cell voltage decreases, it decreases the energy required for hydrogen production, resulting in better cell performance.

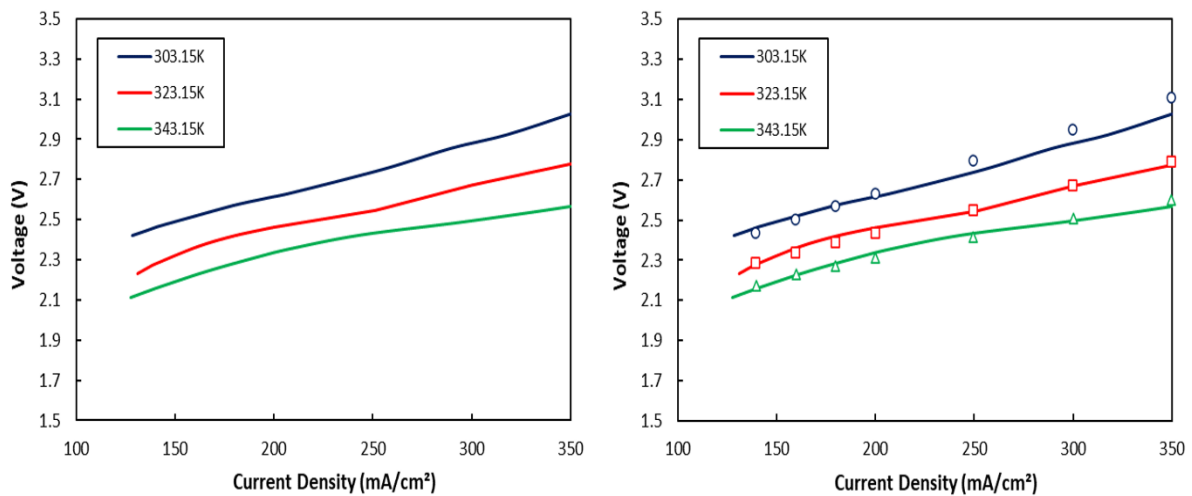


Figure 6.1: Polarization curves 30°C, 50°C and 70°C were generated and validated with experimental data. Model results are represented by lines and experimental data by dots.

6.2.2 Influence of Electrolyte weight concentration

Another important parameter that has a significant effect on the Alkaline water electrolysis cell's performance is the KOH electrolyte weight concentration. At 22wt% and 32wt% electrolyte weight concentrations, the polarization curves were generated to simulate its effects on the AWE cell. In figure 11, the model results were validated against the experimental data and shows minimal error. The voltage of the AWE decreases as the electrolyte concentrations increases because the electrochemical reactions occurring in AWE cell initially require a sufficiently high electrolyte concentration to occur. As the concentration keeps on increasing, the conductivity of the electrolyte also increases, and this leads to a decrease in the required cell voltage, hence reducing the energy needed. Once a required concentration is reached, any further increase will then reduce the electrolyte conductivity

because of the excess ions in the solution. The electrolyte conductivity at 32wt% and 22wt% KOH is found out to be 94.54 S/m and 90.80 S/m respectively.

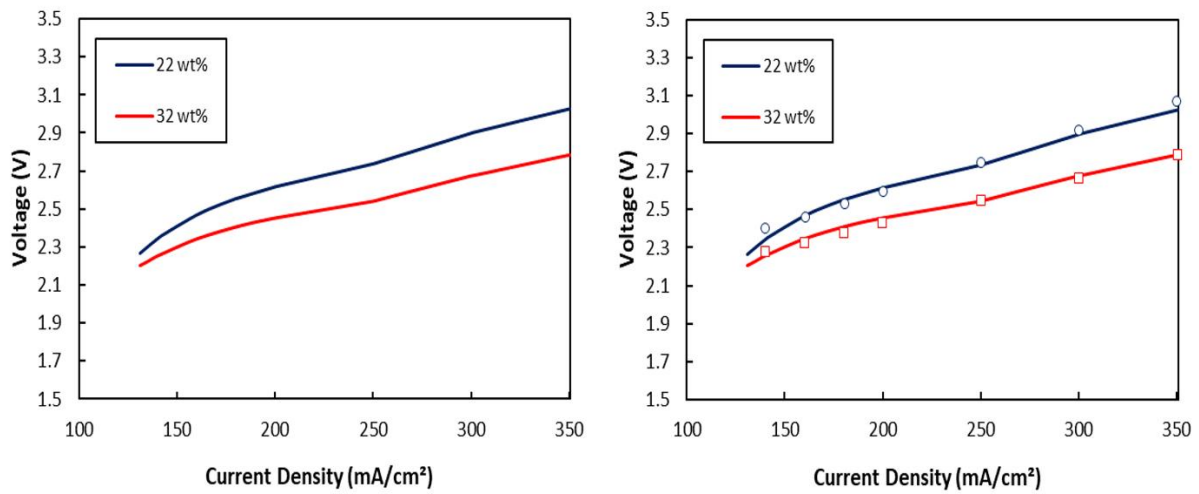


Figure 6.2: Polarization curves at 22wt% and 32wt% KOH electrolyte weight concentrations are generated and validated with experimental data. Model results are represented by lines and experimental data by dots.

6.2.3 Influence of Electrode-Diaphragm distance

Polarization curves were generated at 10mm, 4mm and 1.5mm electrode-diaphragm distances to simulate its influence on the AWE cell's performance while keeping other conditions the same as discussed earlier for temperature. The CFD model results at these operating conditions were validated against the experimental data as shown in figure 12. It was noticed that the cell voltage decreases as the distance between the electrodes and diaphragm decreases. Due to this, efficiency is increased and a drop in total required energy is seen because of the free movement of the ions in cell.

Also, when the cell's distance is very less, it leads to high values of gas fraction resulting in the production of non-conductive gases and high overpotential values. The overall conductivity of the cell is reduced, and a higher value of electrical potential will be required to maintain the same level of performance. This concludes that there exists an optimal electrode-diaphragm distance for achieving maximum overall efficiency.

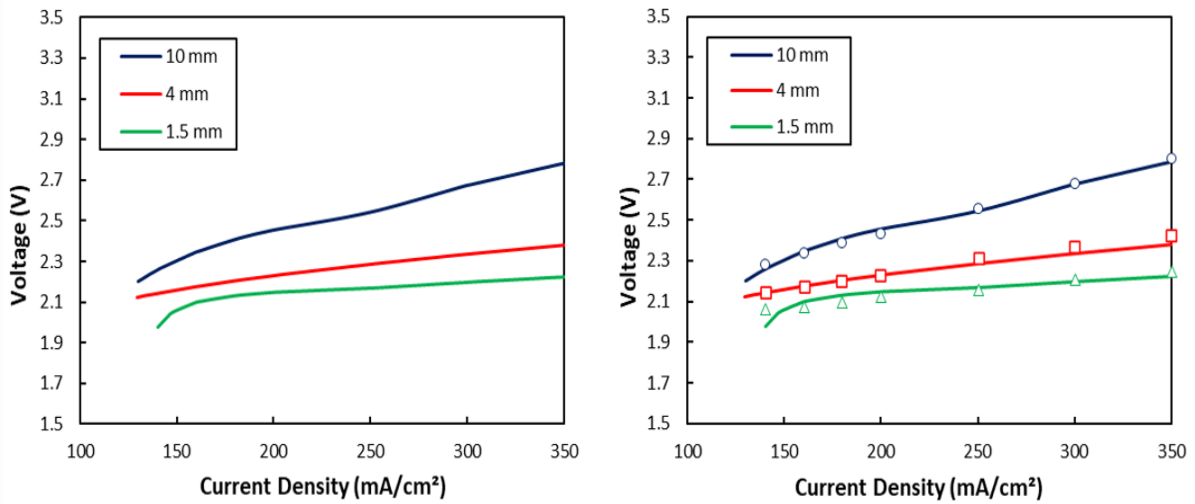


Figure 6.3: Polarization curves are generated at 10mm, 4mm, and 1.5mm electrode-diaphragm distance, and then validated with experimental data. Model results are represented by lines and experimental data by dots.

6.3 Gas Generation Profile

Gas distributions in the electrodes of the cell were simulated on COMSOL and shown in figure 13, this helps in understanding the performance of the AWE cell and optimizing its operating conditions. The electrodes are represented as "thick rectangles" with a width of 1.5, 4 and 10mm while the diaphragm's width is set as 0.5 mm. The gas contour in the figure provides valuable insights into the spatial distribution of the generated gases in the cell, which is crucial for understanding the electrochemical processes and optimizing the cell's performance for efficient hydrogen production.

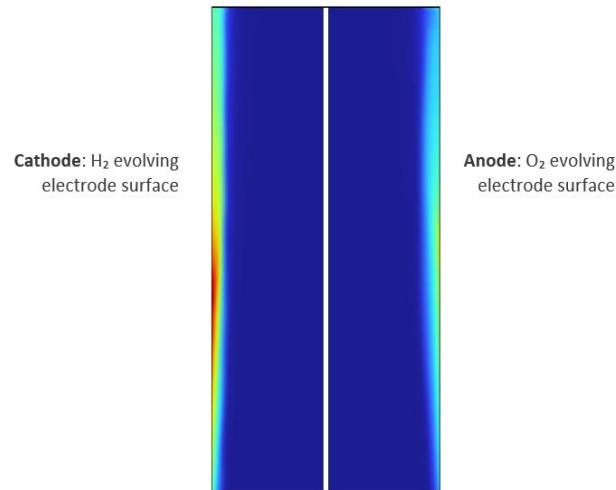


Figure 6.4: Gas distributions in the AWE cell.

6.4 AWE Cell's Performance Evaluation Using Artificial Neural Network

Alkaline water electrolysis involves water splitting technique for hydrogen production, in which electricity is passed between the electrodes to split water molecules into hydrogen and oxygen gas. Temperature, electrolyte weight concentration, electrode-diaphragm distance, bubble size, cell voltage, velocity, and porosity were among the factors affecting the efficiency of AWE. ML techniques such as ANN were employed to improve the efficiency and performance of AWE, simply by analyzing and predicting the relationship between the input and output parameters. In this thesis, a 2D AWE cell was simulated using COMSOL MULTIPHYSICS 6.1 and validated with experimental data. Then, a parametric sweep was applied to generate datasets. The datasets were then exported to MATLAB in order to train a neural network in order to accurately predict the AWE cell's performance. The datasets were divided into three different categories, 70% of the datasets were used for training, 20% for testing and 10% for validation. Lastly, an artificial neural network model was trained and validated using neural network toolbox in MATLAB [53], [76]. The ANN model's performance was evaluated with the help of regression plots as shown in figure 14. Regression plots illustrate the data provided to MATLAB was accurately trained with an overall R value of 0.99922.

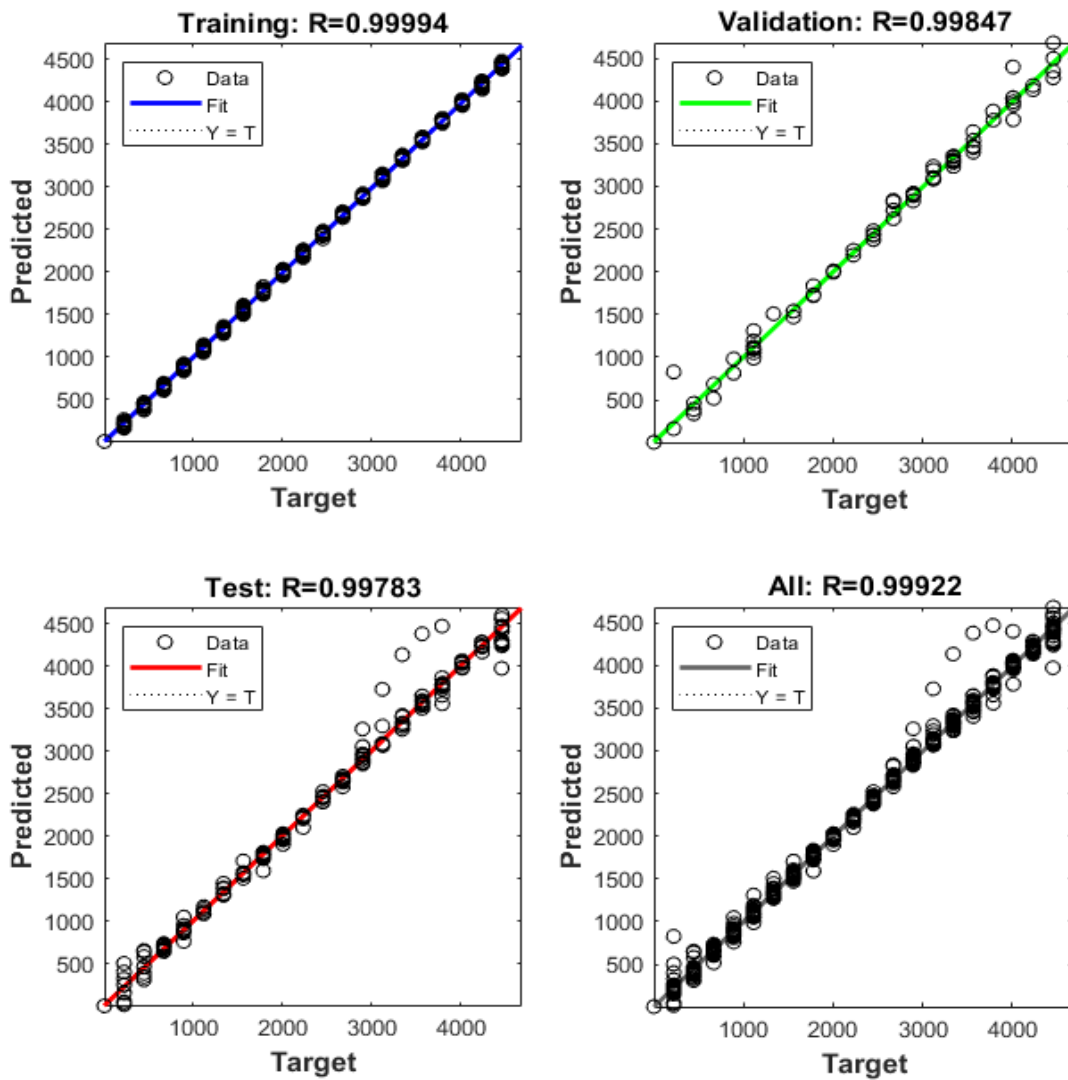


Figure 6.5: Regression plots of ANN model showing target vs. predicted values.

6.5 Analysis of ANN Model Accuracy and Validation

The datasets generated using different values of temperature, current density, and KOH electrolyte conductivity on COMSOL MULTIPHYSICS were used to train the ANN model. The neural network was trained using Levenberg Marquardt training algorithm. The input layer consists of three variables (temperature, current density, electrolyte weight concentration) and the output layer was used for the accurate prediction of the voltage and current density in correspondence to the operating parameters.

The ANN model is trained and to ensure the capabilities to learn the complex patterns and relationships between the input parameters and the target variables, validation of the ANN model is performed. The validation is an important step to ensure ANN's predictive accuracy. The input parametric data was provided to MATLAB and the output data was generated as targets by the developed optimized network. The predicted results of the ANN model were then compared to the COMSOL results. Figure 15 illustrates the ANN model results align closely with the COMSOL output data.

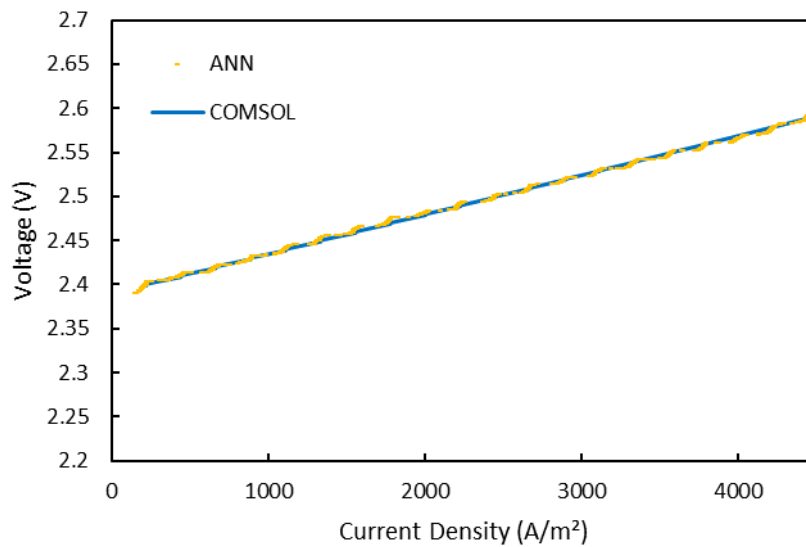


Figure 6.6: Comparison Plots of ANN and CFD Model.

CHAPTER 7: CONCLUSION

In this work, a 2D alkaline water electrolysis model was simulated on COMSOL MULTIPHYSICS. The electrochemical and fluid dynamic responses were evaluated to gain better understanding of the AWE cell's behavior and enhance its performance. The CFD model predicted the distribution of the generated gases, movement of the bubbles, and turbulence within the cell as well as the impact of current density, electrolyte flow rate, electrode-diaphragm distance, and other parameters on the gas profiles. The model results were validated with experimental data through the help of polarization curves. A neural network model was trained using the CFD datasets, and an R^2 value of 0.99922 was achieved. The combined CFD-ANN approach was implemented to optimize the cell's design and performance. The AWE cell showed better performance when small electrode-diaphragm distances, high temperatures and electrolyte weight concentrations were used. The cross validation between CFD and ANN models enhanced the accuracy and reliability of results. Future research work should be focused on developing complex CFD models and integrating them with advanced machine learning algorithms for better design and optimization of the AWE cells to accelerate the transition towards a sustainable hydrogen economy.

REFERENCES

- [1] N. Armaroli and V. Balzani, “Solar Electricity and Solar Fuels: Status and Perspectives in the Context of the Energy Transition,” *Chem. – Eur. J.*, vol. 22, no. 1, pp. 32–57, 2016, doi: 10.1002/chem.201503580.
- [2] J. Milewski, G. Guandalini, and S. Campanari, “Modeling an alkaline electrolysis cell through reduced-order and loss-estimate approaches,” *J. Power Sources*, vol. 269, pp. 203–211, Dec. 2014, doi: 10.1016/j.jpowsour.2014.06.138.
- [3] C. E. McGlade, “A review of the uncertainties in estimates of global oil resources,” *Energy*, vol. 47, no. 1, pp. 262–270, Nov. 2012, doi: 10.1016/j.energy.2012.07.048.
- [4] R. J. Norby and Y. Luo, “Evaluating ecosystem responses to rising atmospheric CO₂ and global warming in a multi-factor world,” *New Phytol.*, vol. 162, no. 2, pp. 281–293, 2004, doi: 10.1111/j.1469-8137.2004.01047.x.
- [5] X. Cheng *et al.*, “A review of PEM hydrogen fuel cell contamination: Impacts, mechanisms, and mitigation,” *J. Power Sources*, vol. 165, no. 2, pp. 739–756, Mar. 2007, doi: 10.1016/j.jpowsour.2006.12.012.
- [6] W. C. Lattin and V. P. Utgikar, “Transition to hydrogen economy in the United States: A 2006 status report,” *Int. J. Hydrog. Energy*, vol. 32, no. 15, pp. 3230–3237, Oct. 2007, doi: 10.1016/j.ijhydene.2007.02.004.
- [7] S. W. Sharshir, A. Joseph, M. M. Elsayad, A. A. Tareemi, A. W. Kandeal, and M. R. Elkadeem, “A review of recent advances in alkaline electrolyzer for green hydrogen production: Performance improvement and applications,” *Int. J. Hydrog. Energy*, vol. 49, pp. 458–488, Jan. 2024, doi: 10.1016/j.ijhydene.2023.08.107.
- [8] D. M. F. Santos, C. A. C. Sequeira, and J. L. Figueiredo, “Hydrogen production by alkaline water electrolysis,” *Quím. Nova*, vol. 36, pp. 1176–1193, 2013, doi: 10.1590/S0100-40422013000800017.
- [9] M. Wang, Z. Wang, X. Gong, and Z. Guo, “The intensification technologies to water electrolysis for hydrogen production – A review,” *Renew. Sustain. Energy Rev.*, vol. 29, pp. 573–588, Jan. 2014, doi: 10.1016/j.rser.2013.08.090.
- [10] E. Amores, J. Rodríguez, J. Oviedo, and A. de Lucas-Consuegra, “Development of an operation strategy for hydrogen production using solar PV energy based on fluid dynamic aspects,” *Open Eng.*, vol. 7, no. 1, pp. 141–152, Jan. 2017, doi: 10.1515/eng-2017-0020.
- [11] F. Z. Aouali, M. Becherif, H. S. Ramadan, M. Emziane, A. Khellaf, and K. Mohammedi, “Analytical modelling and experimental validation of proton exchange membrane electrolyser for hydrogen production,” *Int. J. Hydrog. Energy*, vol. 42, no. 2, pp. 1366–1374, Jan. 2017, doi: 10.1016/j.ijhydene.2016.03.101.

- [12] A. Ursua, L. M. Gandia, and P. Sanchis, “Hydrogen Production From Water Electrolysis: Current Status and Future Trends,” *Proc. IEEE*, vol. 100, no. 2, pp. 410–426, Feb. 2012, doi: 10.1109/JPROC.2011.2156750.
- [13] “Green hydrogen cost reduction: Scaling up electrolyzers to meet the 1.5C climate goal. IRENA, 2020.”.
- [14] M. Sánchez, E. Amores, L. Rodríguez, and C. Clemente-Jul, “Semi-empirical model and experimental validation for the performance evaluation of a 15 kW alkaline water electrolyzer,” *Int. J. Hydrog. Energy*, vol. 43, no. 45, pp. 20332–20345, Nov. 2018, doi: 10.1016/j.ijhydene.2018.09.029.
- [15] S. A. Grigoriev, V. N. Fateev, D. G. Bessarabov, and P. Millet, “Current status, research trends, and challenges in water electrolysis science and technology,” *Int. J. Hydrog. Energy*, vol. 45, no. 49, pp. 26036–26058, Oct. 2020, doi: 10.1016/j.ijhydene.2020.03.109.
- [16] J. Wang *et al.*, “Non-precious-metal catalysts for alkaline water electrolysis: operando characterizations, theoretical calculations, and recent advances,” *Chem. Soc. Rev.*, vol. 49, no. 24, pp. 9154–9196, Dec. 2020, doi: 10.1039/D0CS00575D.
- [17] H. Teuku, I. Alshami, J. Goh, M. S. Masdar, and K. S. Loh, “Review on bipolar plates for low-temperature polymer electrolyte membrane water electrolyzer,” *Int. J. Energy Res.*, vol. 45, no. 15, pp. 20583–20600, 2021, doi: 10.1002/er.7182.
- [18] Y. Yang *et al.*, “The scheduling of alkaline water electrolysis for hydrogen production using hybrid energy sources,” *Energy Convers. Manag.*, vol. 257, p. 115408, Apr. 2022, doi: 10.1016/j.enconman.2022.115408.
- [19] C. T. Bowen, H. J. Davis, B. F. Henshaw, R. Lachance, R. L. LeRoy, and R. Renaud, “Developments in advanced alkaline water electrolysis,” *Int. J. Hydrog. Energy*, vol. 9, no. 1, pp. 59–66, Jan. 1984, doi: 10.1016/0360-3199(84)90032-6.
- [20] D. Parra, L. Valverde, F. J. Pino, and M. K. Patel, “A review on the role, cost and value of hydrogen energy systems for deep decarbonisation,” *Renew. Sustain. Energy Rev.*, vol. 101, pp. 279–294, Mar. 2019, doi: 10.1016/j.rser.2018.11.010.
- [21] “Deiman, J. R., & van Troostwijk, A. P. (1789). Lettre a M. de la Metherie. *J. Phys. Chim. L’hist. Nat*, 35, 369-378.”.
- [22] M. Chatenet *et al.*, “Water electrolysis: from textbook knowledge to the latest scientific strategies and industrial developments,” *Chem. Soc. Rev.*, vol. 51, no. 11, pp. 4583–4762, Jun. 2022, doi: 10.1039/D0CS01079K.

- [23] P. Olivier, C. Bourasseau, and Pr. B. Bouamama, “Low-temperature electrolysis system modelling: A review,” *Renew. Sustain. Energy Rev.*, vol. 78, pp. 280–300, Oct. 2017, doi: 10.1016/j.rser.2017.03.099.
- [24] K. Zeng and D. Zhang, “Recent progress in alkaline water electrolysis for hydrogen production and applications,” *Prog. Energy Combust. Sci.*, vol. 36, no. 3, pp. 307–326, Jun. 2010, doi: 10.1016/j.pecs.2009.11.002.
- [25] M. David, C. Ocampo-Martínez, and R. Sánchez-Peña, “Advances in alkaline water electrolyzers: A review,” *J. Energy Storage*, vol. 23, pp. 392–403, Jun. 2019, doi: 10.1016/j.est.2019.03.001.
- [26] M. Hammoudi, C. Henao, K. Agbossou, Y. Dubé, and M. L. Doumbia, “New multi-physics approach for modelling and design of alkaline electrolyzers,” *Int. J. Hydrog. Energy*, vol. 37, no. 19, pp. 13895–13913, Oct. 2012, doi: 10.1016/j.ijhydene.2012.07.015.
- [27] A. Buttler and H. Spliethoff, “Current status of water electrolysis for energy storage, grid balancing and sector coupling via power-to-gas and power-to-liquids: A review,” *Renew. Sustain. Energy Rev.*, vol. 82, pp. 2440–2454, Feb. 2018, doi: 10.1016/j.rser.2017.09.003.
- [28] C. Varela, M. Mostafa, and E. Zondervan, “Modeling alkaline water electrolysis for power-to-x applications: A scheduling approach,” *Int. J. Hydrog. Energy*, vol. 46, no. 14, pp. 9303–9313, Feb. 2021, doi: 10.1016/j.ijhydene.2020.12.111.
- [29] N. A. Burton, R. V. Padilla, A. Rose, and H. Habibullah, “Increasing the efficiency of hydrogen production from solar powered water electrolysis,” *Renew. Sustain. Energy Rev.*, vol. 135, p. 110255, Jan. 2021, doi: 10.1016/j.rser.2020.110255.
- [30] K. Hu *et al.*, “Comparative study of alkaline water electrolysis, proton exchange membrane water electrolysis and solid oxide electrolysis through multiphysics modeling,” *Appl. Energy*, vol. 312, p. 118788, Apr. 2022, doi: 10.1016/j.apenergy.2022.118788.
- [31] “Water electrolysis based on renewable energy for hydrogen production - ScienceDirect.” Accessed: Dec. 13, 2023. [Online]. Available: https://www.sciencedirect.com/science/article/pii/S1872206717629498?casa_token=yxzfzvWILYAAAAA:oARIJb74Kh9T5zDsFK0-TT9130ax-J8EYmeHL9ojPMNAHVHuhGrcfYkmJZ3ISL72yUORX0chrkbg
- [32] E. Amores, J. Rodríguez, and C. Carreras, “Influence of operation parameters in the modeling of alkaline water electrolyzers for hydrogen production,” *Int. J. Hydrog. Energy*, vol. 39, no. 25, pp. 13063–13078, Aug. 2014, doi: 10.1016/j.ijhydene.2014.07.001.
- [33] M. Carmo, D. L. Fritz, J. Mergel, and D. Stolten, “A comprehensive review on PEM water electrolysis,” *Int. J. Hydrog. Energy*, vol. 38, no. 12, pp. 4901–4934, Apr. 2013, doi: 10.1016/j.ijhydene.2013.01.151.

- [34] O. Schmidt, A. Gambhir, I. Staffell, A. Hawkes, J. Nelson, and S. Few, “Future cost and performance of water electrolysis: An expert elicitation study,” *Int. J. Hydrog. Energy*, vol. 42, no. 52, pp. 30470–30492, Dec. 2017, doi: 10.1016/j.ijhydene.2017.10.045.
- [35] M. A. Laguna-Bercero, “Recent advances in high temperature electrolysis using solid oxide fuel cells: A review,” *J. Power Sources*, vol. 203, pp. 4–16, Apr. 2012, doi: 10.1016/j.jpowsour.2011.12.019.
- [36] “Progress Report on Proton Conducting Solid Oxide Electrolysis Cells - Lei - 2019 - Advanced Functional Materials - Wiley Online Library.” Accessed: Dec. 13, 2023. [Online]. Available: https://onlinelibrary.wiley.com/doi/abs/10.1002/adfm.201903805?casa_token=ehDflhKX6z0AAA:AAA:s780yW7s6_e4je8GebcRvBIbrnB2A4N7rMWiJO57qPkbW9zeQPZJreK-SACZAsLT-9cCKuQJj47dk5lpWQ
- [37] S. Hu *et al.*, “A comprehensive review of alkaline water electrolysis mathematical modeling,” *Appl. Energy*, vol. 327, p. 120099, Dec. 2022, doi: 10.1016/j.apenergy.2022.120099.
- [38] Ø. Ulleberg, “Modeling of advanced alkaline electrolyzers: a system simulation approach,” *Int. J. Hydrog. Energy*, vol. 28, no. 1, pp. 21–33, Jan. 2003, doi: 10.1016/S0360-3199(02)00033-2.
- [39] P. M. Diéguez, A. Ursúa, P. Sanchis, C. Sopena, E. Guelbenzu, and L. M. Gandía, “Thermal performance of a commercial alkaline water electrolyzer: Experimental study and mathematical modeling,” *Int. J. Hydrog. Energy*, vol. 33, no. 24, pp. 7338–7354, Dec. 2008, doi: 10.1016/j.ijhydene.2008.09.051.
- [40] K. C. Sandeep *et al.*, “Experimental studies and modeling of advanced alkaline water electrolyser with porous nickel electrodes for hydrogen production,” *Int. J. Hydrog. Energy*, vol. 42, no. 17, pp. 12094–12103, Apr. 2017, doi: 10.1016/j.ijhydene.2017.03.154.
- [41] E. Amores, J. Ruiz, C. Rodríguez, and P. Escibano, *Study of an Alkaline Electrolyzer Powered by Renewable Energy*. 2011.
- [42] J. Rodríguez and E. Amores, “CFD Modeling and Experimental Validation of an Alkaline Water Electrolysis Cell for Hydrogen Production,” *Processes*, vol. 8, no. 12, Art. no. 12, Dec. 2020, doi: 10.3390/pr8121634.
- [43] A. Zarghami, N. G. Deen, and A. W. Vreman, “CFD modeling of multiphase flow in an alkaline water electrolyzer,” *Chem. Eng. Sci.*, vol. 227, p. 115926, Dec. 2020, doi: 10.1016/j.ces.2020.115926.
- [44] K. Stewart *et al.*, “Modeling and Optimization of an Alkaline Water Electrolysis for Hydrogen Production,” in *2021 IEEE Green Energy and Smart Systems Conference (IGESSC)*, Nov. 2021, pp. 1–6. doi: 10.1109/IGESSC53124.2021.9618679.

- [45] G. Hawkes, J. O'Brien, C. Stoots, and B. Hawkes, "3D CFD model of a multi-cell high-temperature electrolysis stack," *Int. J. Hydrog. Energy*, vol. 34, no. 9, pp. 4189–4197, May 2009, doi: 10.1016/j.ijhydene.2008.11.068.
- [46] M. D. Mat, K. Aldas, and O. J. Ilegbusi, "A two-phase flow model for hydrogen evolution in an electrochemical cell," *Int. J. Hydrog. Energy*, vol. 29, no. 10, pp. 1015–1023, Aug. 2004, doi: 10.1016/j.ijhydene.2003.11.007.
- [47] M. O. K. Mendonça, S. L. Netto, P. S. R. Diniz, and S. Theodoridis, "Chapter 13 - Machine learning: Review and trends," in *Signal Processing and Machine Learning Theory*, P. S. R. Diniz, Ed., Academic Press, 2024, pp. 869–959. doi: 10.1016/B978-0-32-391772-8.00019-3.
- [48] D. Sen, K. M. M. Tunç, and M. E. Günay, "Forecasting electricity consumption of OECD countries: A global machine learning modeling approach," *Util. Policy*, vol. 70, p. 101222, Jun. 2021, doi: 10.1016/j.jup.2021.101222.
- [49] X. Liu, B. Moreno, and A. S. García, "A grey neural network and input-output combined forecasting model. Primary energy consumption forecasts in Spanish economic sectors," *Energy*, vol. 115, pp. 1042–1054, Nov. 2016, doi: 10.1016/j.energy.2016.09.017.
- [50] A. Sohani *et al.*, "Using machine learning in photovoltaics to create smarter and cleaner energy generation systems: A comprehensive review," *J. Clean. Prod.*, vol. 364, p. 132701, Sep. 2022, doi: 10.1016/j.jclepro.2022.132701.
- [51] E. Zhao, S. Sun, and S. Wang, "New developments in wind energy forecasting with artificial intelligence and big data: a scientometric insight," *Data Sci. Manag.*, vol. 5, no. 2, pp. 84–95, Jun. 2022, doi: 10.1016/j.dsm.2022.05.002.
- [52] S. Safarian, S. M. Ebrahimi Saryazdi, R. Unnthorsson, and C. Richter, "Modeling of Hydrogen Production by Applying Biomass Gasification: Artificial Neural Network Modeling Approach," *Fermentation*, vol. 7, no. 2, Art. no. 2, Jun. 2021, doi: 10.3390/fermentation7020071.
- [53] A. Zamaniyan, F. Joda, A. Behroozsarand, and H. Ebrahimi, "Application of artificial neural networks (ANN) for modeling of industrial hydrogen plant," *Int. J. Hydrog. Energy*, vol. 38, no. 15, pp. 6289–6297, May 2013, doi: 10.1016/j.ijhydene.2013.02.136.
- [54] M.-A. Babay, M. Adar, A. Chebak, and M. Mabrouki, "Dynamics of Gas Generation in Porous Electrode Alkaline Electrolysis Cells: An Investigation and Optimization Using Machine Learning," *Energies*, vol. 16, no. 14, Art. no. 14, Jan. 2023, doi: 10.3390/en16145365.
- [55] "Alkaline Electrolysers - an overview | ScienceDirect Topics." Accessed: Nov. 22, 2023. [Online]. Available: <https://www.sciencedirect.com/topics/engineering/alkaline-electrolysers>
- [56] P. Haug, M. Koj, and T. Turek, "Influence of process conditions on gas purity in alkaline water electrolysis," *Int. J. Hydrog. Energy*, vol. 42, no. 15, pp. 9406–9418, Apr. 2017, doi: 10.1016/j.ijhydene.2016.12.111.

- [57] J. Brauns *et al.*, “Evaluation of Diaphragms and Membranes as Separators for Alkaline Water Electrolysis,” *J. Electrochem. Soc.*, vol. 168, no. 1, 2021, doi: 10.1149/1945-7111/abda57.
- [58] S. Krishnan, M. Fairlie, P. Andres, T. de Groot, and G. Jan Kramer, “Chapter 10 - Power to gas (H₂): alkaline electrolysis,” in *Technological Learning in the Transition to a Low-Carbon Energy System*, M. Junginger and A. Louwen, Eds., Academic Press, 2020, pp. 165–187. doi: 10.1016/B978-0-12-818762-3.00010-8.
- [59] D. Huang *et al.*, “A multiphysics model of the compactly-assembled industrial alkaline water electrolysis cell,” *Appl. Energy*, vol. 314, p. 118987, May 2022, doi: 10.1016/j.apenergy.2022.118987.
- [60] “A numerical simulation to effectively assess impacts of flow channels characteristics on solid oxide fuel cell performance - ScienceDirect.” Accessed: Dec. 15, 2023. [Online]. Available: https://www.sciencedirect.com/science/article/pii/S0196890421004568?casa_token=uR9anHjzceEAAAAA:w5KzG7_GS5wIm3OjXomA4GiGG3MUrqFB5A-CJ5rxWMyfUZTIKPctPEbHL-13v88eUWuBums6OTJo
- [61] J. Rodríguez, S. Palmas, M. Sánchez-Molina, E. Amores, L. Mais, and R. Campana, “Simple and Precise Approach for Determination of Ohmic Contribution of Diaphragms in Alkaline Water Electrolysis,” *Membranes*, vol. 9, no. 10, Art. no. 10, Oct. 2019, doi: 10.3390/membranes9100129.
- [62] M. F. Kibria, M. Sh. Mridha, and A. H. Khan, “Electrochemical studies of a nickel electrode for the hydrogen evolution reaction,” *Int. J. Hydrog. Energy*, vol. 20, no. 6, pp. 435–440, Jun. 1995, doi: 10.1016/0360-3199(94)00073-9.
- [63] M. F. Kibria and M. Sh. Mridha, “Electrochemical studies of the nickel electrode for the oxygen evolution reaction,” *Int. J. Hydrog. Energy*, vol. 21, no. 3, pp. 179–182, Mar. 1996, doi: 10.1016/0360-3199(95)00066-6.
- [64] R. J. Gilliam, J. W. Graydon, D. W. Kirk, and S. J. Thorpe, “A review of specific conductivities of potassium hydroxide solutions for various concentrations and temperatures,” *Int. J. Hydrog. Energy*, vol. 32, no. 3, pp. 359–364, Mar. 2007, doi: 10.1016/j.ijhydene.2006.10.062.
- [65] M. P. M. G. WEIJS, L. J. J. JANSSEN, and G. J. VISSER, “Ohmic resistance of solution in a vertical gas-evolving cell,” *J. Appl. Electrochem.*, vol. 27, no. 4, pp. 371–378, Apr. 1997, doi: 10.1023/A:1018449301423.
- [66] R. L. LeRoy, C. T. Bowen, and D. J. LeRoy, “The Thermodynamics of Aqueous Water Electrolysis,” *J. Electrochem. Soc.*, vol. 127, no. 9, p. 1954, Sep. 1980, doi: 10.1149/1.2130044.
- [67] J. O. B. Lira, H. G. Riella, N. Padoin, and C. Soares, “Computational fluid dynamics (CFD), artificial neural network (ANN) and genetic algorithm (GA) as a hybrid method for the analysis and optimization of micro-photocatalytic reactors: NO_x abatement as a case study,” *Chem. Eng. J.*, vol. 431, p. 133771, Mar. 2022, doi: 10.1016/j.cej.2021.133771.

- [68] R. Y. Choi, A. S. Coyner, J. Kalpathy-Cramer, M. F. Chiang, and J. P. Campbell, “Introduction to Machine Learning, Neural Networks, and Deep Learning,” *Transl. Vis. Sci. Technol.*, vol. 9, no. 2, p. 14, doi: 10.1167/tvst.9.2.14.
- [69] A. Holzinger, M. Plass, K. Holzinger, G. C. Crisan, C.-M. Pintea, and V. Palade, “A glass-box interactive machine learning approach for solving NP-hard problems with the human-in-the-loop.” arXiv, Aug. 03, 2017. doi: 10.48550/arXiv.1708.01104.
- [70] I. H. Sarker, “Deep Learning: A Comprehensive Overview on Techniques, Taxonomy, Applications and Research Directions,” *SN Comput. Sci.*, vol. 2, no. 6, p. 420, Aug. 2021, doi: 10.1007/s42979-021-00815-1.
- [71] M. van Gerven and S. Bohte, “Editorial: Artificial Neural Networks as Models of Neural Information Processing,” *Front. Comput. Neurosci.*, vol. 11, 2017, Accessed: Dec. 17, 2023. [Online]. Available: <https://www.frontiersin.org/articles/10.3389/fncom.2017.00114>
- [72] “An Introduction to Statistical Learning,” An Introduction to Statistical Learning. Accessed: Dec. 17, 2023. [Online]. Available: <https://www.statlearning.com>
- [73] “(5) The Elements of Statistical Learning: Data Mining, Inference, and Prediction, Second Edition (Springer Series in Statistics) | Request PDF.” Accessed: Dec. 17, 2023. [Online]. Available: https://www.researchgate.net/publication/319770542_The_Elements_of_Statistical_Learning_Data_Mining_Inference_and_Prediction_Second_Edition_Springer_Series_in_Statistics
- [74] “Categories of Machine Learning Algorithms,” BI / DW Insider. Accessed: Dec. 17, 2023. [Online]. Available: <https://bi-insider.com/posts/categories-of-machine-learning-algorithms/>
- [75] “State-of-the-art in artificial neural network applications: A survey - ScienceDirect.” Accessed: Dec. 18, 2023. [Online]. Available: <https://www.sciencedirect.com/science/article/pii/S2405844018332067>
- [76] G. Di Franco and M. Santurro, “Machine learning, artificial neural networks and social research,” *Qual. Quant.*, vol. 55, no. 3, pp. 1007–1025, Jun. 2021, doi: 10.1007/s11135-020-01037-y.